Abstract

This thesis is primarily focused on the design of broadband microstrip antenna and the technique of mutual coupling reduction between microstrip antenna elements and arrays. A novel broadband antenna is designed, a new technique to reduce the mutual coupling between two antenna elements is pesented and a time-saving method to calculate the mutual coupling between large arrays is proposed.

This thesis firstly describes the design of a novel fork-like stripline-fed aperture coupled antenna element. This antenna is fully planar, and the fork-like feed line is utilized to improve the impedance bandwidth. The nonresonant aperture is used to reduce the backlobe radiation. The measured results show that this antenna element can achieve a broad bandwidth with a low backlobe level and a low cross polarization level.

A novel parasitic structure is inserted between two microstrip antenna elements to reduce the mutual coupling by canceling the space wave. The measured results show that a 13dB mutual coupling reduction is obtained across a broad bandwidth, while the antenna radiation patterns in both E-plane and H-plane remain unaffected.

The network method is used to reduce the calculation time of mutual coupling between two large microstrip antenna arrays. In the network method, the arrays are divided into two parts: the radiating elements and the feeding networks. The element spacing of the arrays along the coupling direction is adjusted to reduce the mutual coupling. The spacing between the centers of two arrays is fixed. By using the network method, the total calculating time is greatly reduced. The mutual coupling level between the adjusted arrays is 10dB lower than that of the original arrays. The adjusted array doesn't show significant degradation of antenna gain and radiation patterns compared with the original array. The simulated and measured results agree well with each other.

Keywords: Microstip Antenna Array, Bandwidth, Stripline-fed, Mutual Coupling, Network method

声　明

本学位论文是我在导师的指导下取得的研究成果，尽我所知，在本学位论文中，除了加以标注和致谢的部分外，不包含其他人已经发表或公布过的研究成果，也不包含我为获得任何教育机构的学位或学历而使用过的材料。与我一同工作的同事对本学位论文做出的贡献均已在论文中作了明确的说明。

研究生签名：_____　　年　月　日

学位论文使用授权声明

南京理工大学有权保存本学位论文的电子和纸质文档，可以借阅或上网公布本学位论文的部分或全部内容，可以向有关部门或机构送交并授权其保存、借阅或上网公布本学位论文的部分或全部内容。对于保密论文，按保密的有关规定和程序处理。

研究生签名：_____　　年　月　日

1 Introduction

1.1 Overview

The microstrip antenna concept was first introduced by Deschamps [1] more than 50 years ago. Since then, Microstrip antennas have become popular for a wide variety of application areas. This is because of their many advantages over conventional antennas, such as being comparably lightweight, low profile, low cost, their conformity to surface and direct integrability with microwave circuitry. On the other hand, compared to the conventional antennas, microstrip antennas have some limitations. These drawbacks are due to its low gain, narrow bandwidth performance and surface waves. Much work has been done to overcome these drawbacks. For example, bandwidth can be increased to more than 100 percent by using special techniques [2]; lower gain and lower power handling limitations can be overcome through an array configuration. Surface wave-associated limitations such as poor efficiency, increased mutual coupling, reduced gain and radiation pattern degradations can be overcome by the use of metal fences [3] or electromagnetic bandgap structures [4].

1.2 Organization of thesis

The following Chapter 2 mainly presents a novel fork-like stripline fed aperture coupled antenna element. The development of aperture coupled antenna is briefly reviewed. And the designed antenna element is fabricated and tested. The simulated and measured results are given for comparison. Chapter 3 mainly discusses the reduction of the mutual coupling between microstrip antenna elements. A novel parasitic structure is inserted between two microstrip antennas to reduce the mutual coupling through canceling the space wave between the two microstrip patch antennas.

Chapter 4 mainly discusses the calculation and reduction of mutual coupling between microstrip antenna arrays. The full wave based network method is used to calculate the mutual coupling. The results of the network method are compared with those calculated by Ansoft Designer. The element spacing along the coupling plane is adjusted to reduce the mutual coupling. Finally the original design and the adjusted design are fabricated and tested.

Chapter 5 summarizes the thesis by reviewing some of the important concepts of this research.

2 A Novel Fork-like Stripline-fed Aperture Coupled Antenna Element

2.1 Literature review

Microstrip antennas are commonly fed by one of three methods: (a) coaxial probe, (b) stripline connected directly to the edge of a patch, and (c) stripline coupled to the patch through an aperture. Feeding by a coaxial probe has the advantages of ease in impedance matching and low spurious radiation and the disadvantage of having to physically connect the center conductor to the patch. The advantage of directly connecting a stripline to the edge of a patch is ease of fabrication. However, impedance matching is not as convenient as the probe feed case, and unwanted radiation from the feed line can be a problem.

A method which has become very popular is to couple energy from the stripline through an aperture (slot) in the ground plane. This method, known as aperture coupling, was first proposed by Pozar [5]. Some of its advantages are as follows: (a) The feed network is isolated from the radiating element by the ground plane which prevents spurious radiation; (b) active devices can be fabricated in a feed substrate with high dielectric constant for size reduction; (c) there are more degrees of freedom for the designer.

The slot that couples energy from the stripline to the patch can be either resonant or nonresonant. If it is resonant, it provides another resonance in operation band. However, the resonant slot has a strong backlobe radiation which substantially reduces the gain of the antenna. For this reason, a nonresonant slot is usually used in aperture coupled microstrip antennas. The impedance bandwidth of the basic form of such antenna is typically 6-7%.

The impedance bandwidth of aperture coupled microstrip antennas can be enhanced by using stacked or coplanar parasitic elements.

An aperture-coupled microstrip stacked patch antenna is studied in [6], with the goal of obtaining wide bandwidth, low cross-polarization and weak parasitic radiation from the feeding aperture for applications in phased array antenna, as is shown in Fig.2.1(a). A 25% bandwidth with VSWR less than 1.6 was achieved. The worst back to front ratio is about -18 dB for this antenna. Another aperture coupled stacked patch antenna with an operating bandwidth (defined as having a return loss of < -10dB) of over 50% is proposed In [7], as is shown Fig.2.1(b). Back radiation levels ranged from -10 to -15dB over the band, relative to

front radiation level.

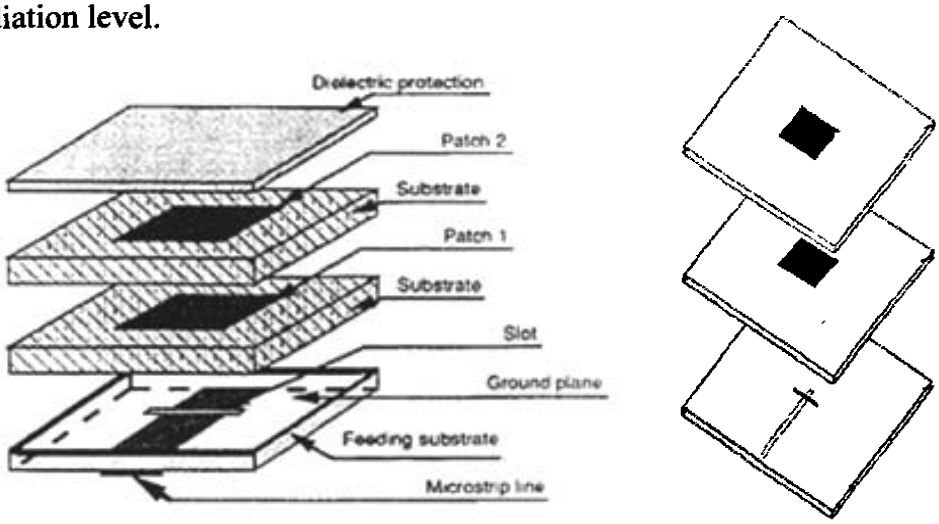

Fig.2.1. (a) The antenna element proposed in [2].
(b) The antenna element proposed in [3].

In [8], coplanar elements are incorporated into the aperture-coupled microstrip antennas. Additional patches are gap-coupled to the nonradiating edges of the fed rectangular patch. The sizes of the additional patches are identical for each configuration. Subarray 1 and subarray 2 have two and four parasitic elements respectively, as is shown in Fig.2.2. The calculated bandwidth of Subarray 1 is about 12%, while that of Subarray 2 is about 17%.

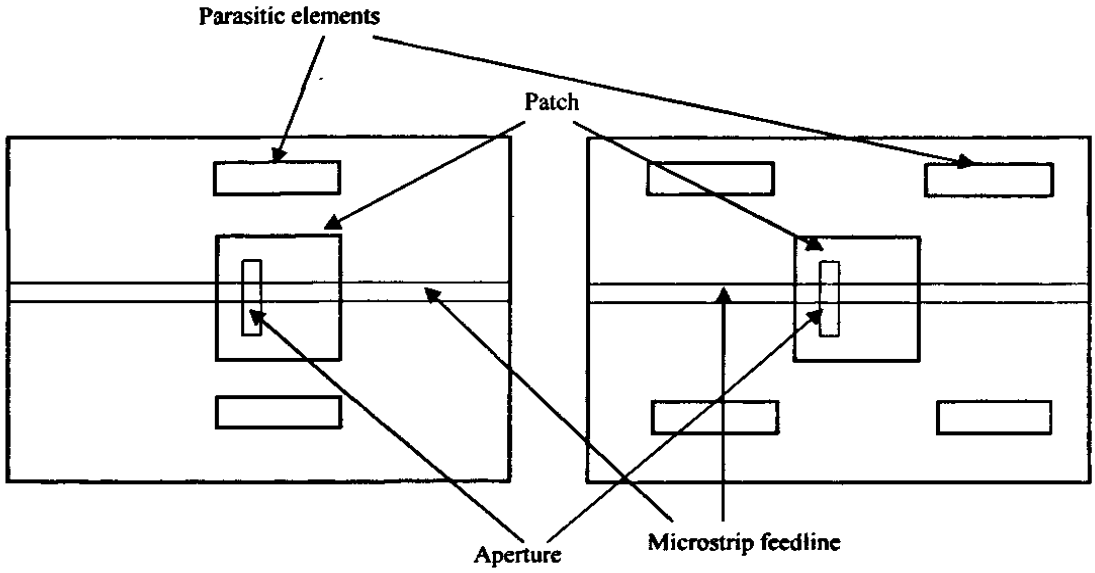

Fig.2.2. (a) The layout of Subarray 1 with 2 parasitic elements
(b) The layout of Subarray 2 with 4 parasitic elements

Two methods commonly used to improve the radiation characteristics are to place a shielding plane behind the antenna in [9] [10] or to enclose the aperture in a cavity in [11].

Both approaches eliminate any unwanted radiation in the back region. However, the incorporation of a shielding plane makes the structure bulky. The use of a cavity eliminates this problem at the expense of greater manufacturing complexity, thereby increasing cost. Another way to improve the front-to-back ratio is to place a microstrip antenna element behind the aperture as a reflector [12], as shown in Fig2.3. Proximity coupling between the feed line and the reflecting element is negligible due to the thick foam substrate used, allowing use of the reciprocity method of analysis. Also, the directive patch elements are shielded from the reflector by the ground plane. Therefore, only interactions between the reflector and the aperture need to be modeled, resulting in a simple analysis, For aperture coupled patch designs with a front-to-back ratio of l0dB or greater, the introduction of a reflecting element has a negligible effect on the input impedance of the antenna. Therefore, a reflector element can readily be incorporated into existing designs.

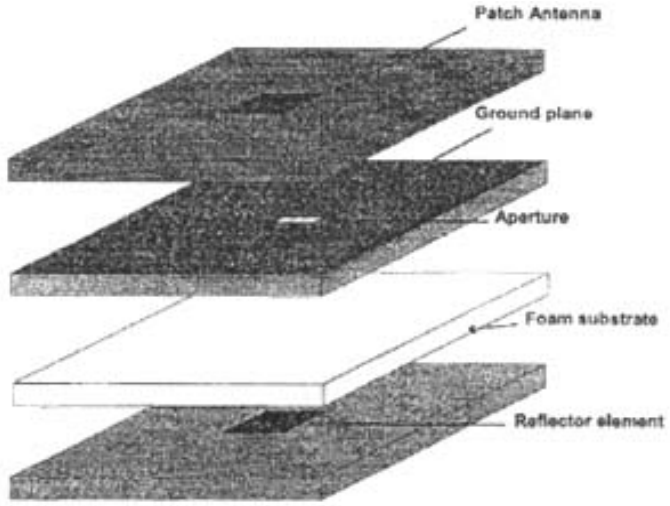

Fig.2.3. Geometry of an aperture coupled microstrip antenna with a reflector element.

Instead of a microstrip feed, a stripline feed is used in [13] [14] and [15] to eliminate the parasitic feed line radiation and the back-radiation of the slot, as is shown in Fig.2.4. The stripline technology allows one to work with antennas having a feed network completely isolated which is very useful for integration in a system containing devices sensitive to parasitic radiations(amplifiers, phase shifters, etc.). This kind of feed line is also very well suited for integration in a multilayer antenna.

The stripline-fed aperture coupled microstrip antenna behaves in a similar manner overall, but with a few additional phenomena to be dealt with. The first involves the currents which return via the ground plane, creating an excitation field in the slot [13]. These currents are now distributed over the two ground planes associated with the feed line. By increasing the height of region 1, the structure tends toward that of a microstrip line, concentrating the

currents on the upper ground plane which enhances the excitation field in the slot, thus improving the resonance of this latter. If regions 2, 3, and 4 in Fig.2.4 are maintained as previously, the real part of the input impedance is seen to increase. The second effect concerns back radiation, which is reduced considerably by the lower ground plane. On the other hand, back radiation from the slot is trapped between the two metallic planes, resulting in the appearance of higher modes. The severity of these parasitic modes depends strongly on the level of back radiation from the slot [16]. These modes can be eliminated by shorting pins between the two ground planes. A two stacked patches structure is used for large bandwidth [14]. This element exhibits a 19.7% band width for an SWR<2 and on-axis cross-polarization < -37dB. The back-radiation level is lower than -25dB over the whole bandwidth.

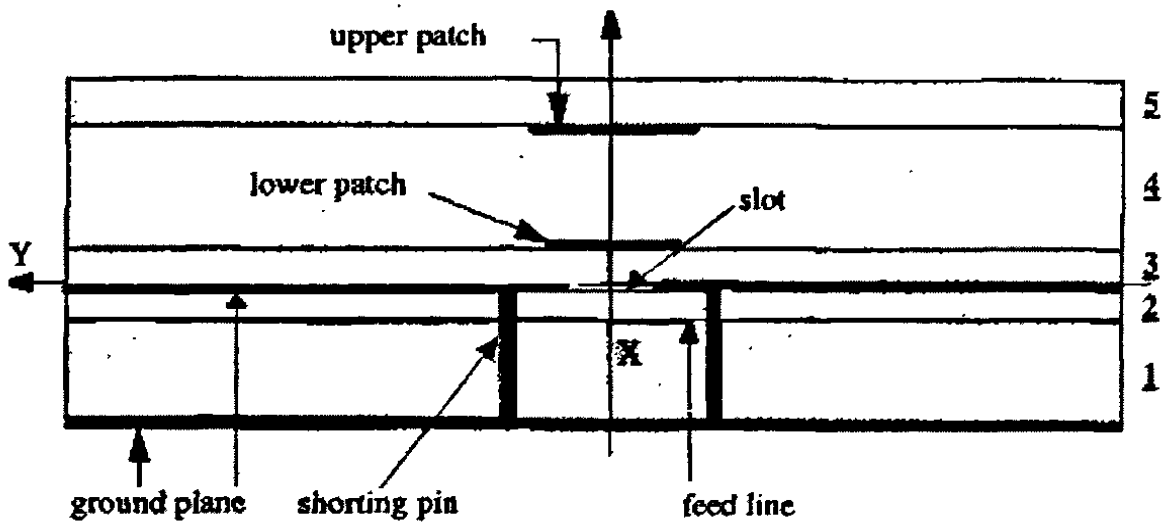

Fig.2.4. Geometry of stripline-fed aperture coupled antenna with vias around the coupling slot

A new stripline-fed, fully planar aperture coupled antenna element designed in the stripline technique without the use of shorting pins or vias around the coupling slot is proposed in [17]. Such strip radiating elements can be easily integrated with feeding networks designed in the most commonly used stripline technique, constituting high performance fully planar large antenna arrays.

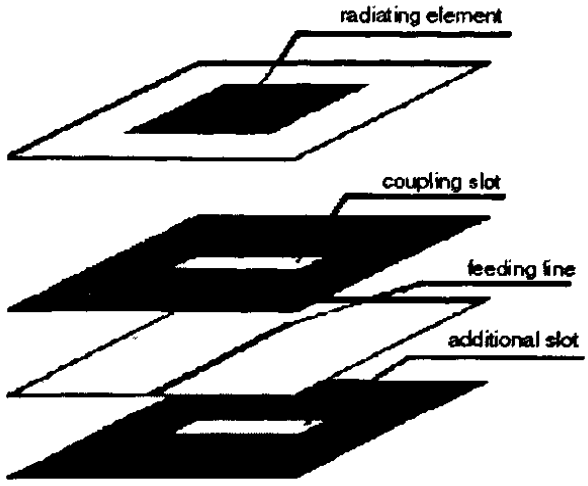

Fig.2.5. Geometry of stripline-fed aperture coupled antenna

Fig. 2.5 shows the stripline-fed aperture coupled antenna element. An air spacer has been inserted between the radiating element and the upper ground plane to ensure appropriate bandwidth of the antenna. The feeding network consists of two layers of laminates, on which the network's strip pattern is etched. The measured gain equals 8 dBi at center frequency. The bandwidth of this element equals 17% for a return loss better than 15 dB.

2.2 A fork-like stripline-fed aperture coupled antenna element

In this section, a novel fork-like stripline-fed aperture coupled antenna element is proposed as depicted in Fig.2.6. This antenna can achieve the wide band performance, the low back radiation levels, and low cross-polarization levels. Compared with the antenna element shown in [17], a novel fork-like feeding structure has been adopted which considerably improves the bandwidth performance. The nonresonant aperture has also been used to suppress the back radiation.

As is shown in Fig.2.6 and Fig.2.7, the antenna is composed of three dielectric layers, four metallization layers and two ground planes. The radiating rectangular patch is etched on the top metallization layer. An air gap is inserted to separate dielectric layer 1 and the upper ground plane. A rectangular coupling aperture is cut in the upper ground plane. The novel fork-like feeding structure is etched between dielectric layer 2 and 3. The lower ground plane is at the bottom, in which a second rectangular aperture is cut.

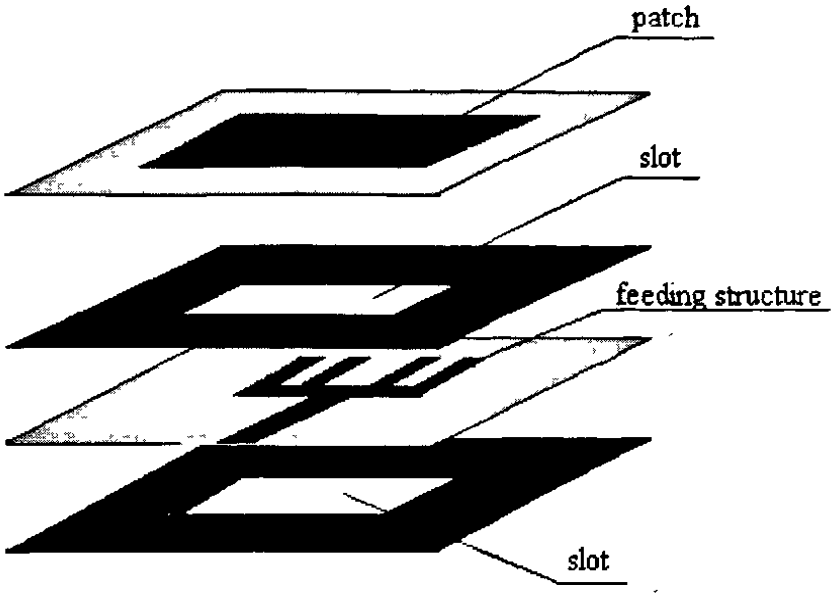

Fig.2.6. Geometry of stripline-fed aperture coupled antenna

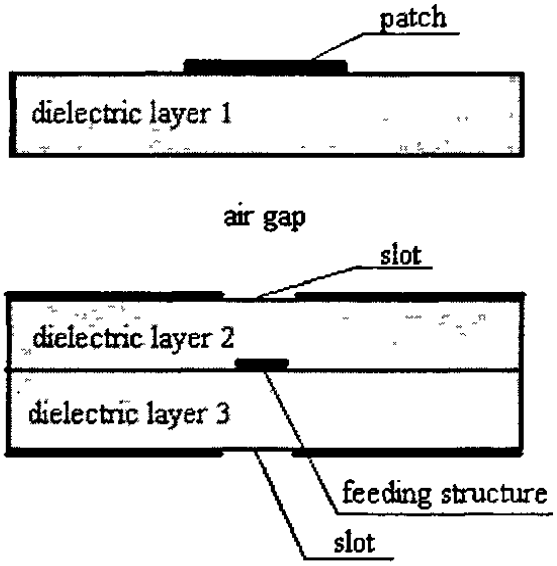

Fig.2.7. Cross-sectional view of the antenna element.

To validate our concept, the antenna element has been designed. As is shown in Fig.2.7, the radiating patch is put on the top of dielectric layer 1 with permittivity ε_r=2.7 and thickness h=0.5mm. The thickness of the air gap is 3.6mm. Dielectric layer 2 has a permittivity of 2.7 and a thickness of 0.5mm, while dielectric layer 3 has a permittivity of 2.7 and a thickness of 1.5mm.

Fig.2.8 shows the basic parameters of radiating patch, coupling aperture, fork-like feeding structure and the aperture in the lower ground plane. The radiating patch has a length

of a_1 and a width of b_1, and the coupling aperture has a length of a_2 and a width of b_2. The second aperture is cut in the lower ground plane with length a_3 and width b_3. The fork-like feeding structure has four branches with equal length w_2 and width w_1, while w_3 is the total width. The distance between every two branches is w_4. Those branches are connected to a 50Ω stripline having a width of w_0.

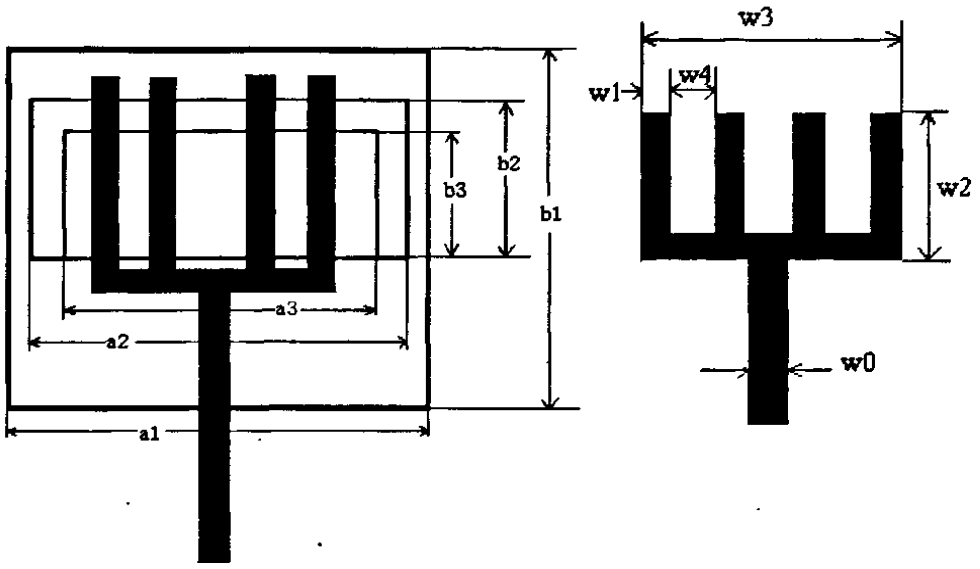

Fig.2.8. Dimensions of the antenna: a_1=12.2mm, a_2=10.6mm, a_3=9.8mm, b_1=12.4mm, b_2=5.4mm, b_3=3.9mm, w_0=1.0mm, w_1=0.8mm, w_2=7.4mm, w_3=7.0mm, w_4=1.5mm.

Fig.2.9 shows the simulated and measured VSWR characteristics of the proposed antenna element. The bandwidth is better than 55%. The frequency range is from 5.7GHz to 10.1GHz (VSWR<2:1). It is interesting to note that, compared to [17], although the bandwidth is narrower for the criterion of VSWR<1.5:1, it is much wider for the criterion of VSWR<2:1. This advantage is caused from the fork-like structure which provides the multi-resonances as is seen in Fig.2.8. The measured antenna gain against frequency is shown in Fig.2.10. The peak gain attains 8dBi around the center frequency. It is shown that the gain bandwidth of this antenna is not as wide as the impedance bandwidth. The antenna gain drops to below 0dBi at the edge frequencies. However, a bandwidth broader than 20% is still obtained for gain over 5dBi. The E-plane and H-plane radiation patterns measured at center frequency 8 GHz are presented in Fig.2.11 and Fig.2.12, separately. The front to back ratio of the antenna radiation pattern is better than 22dB in both planes. The cross polarization level is better than -26dB in E-plane and -27dB in H-plane, respectively. Fig.2.13 shows the fabricated antenna element. All the above simulations are performed by Zeland IE3D V.10.

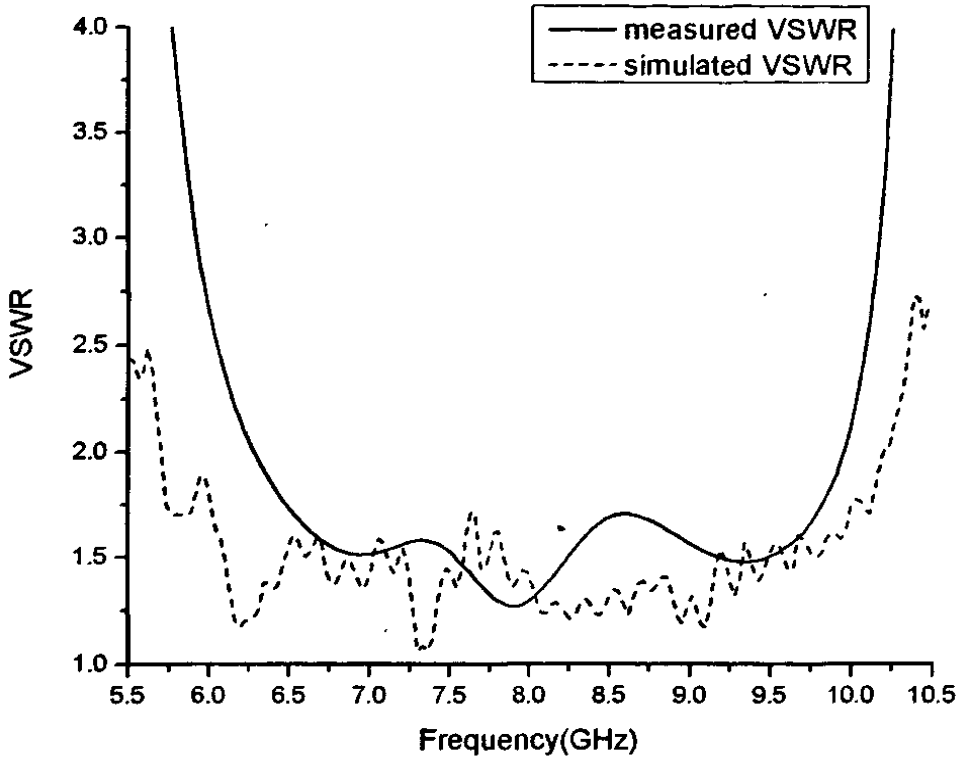

Fig.2.9. The simulated and measured VSWR characteristics of the proposed antenna element.

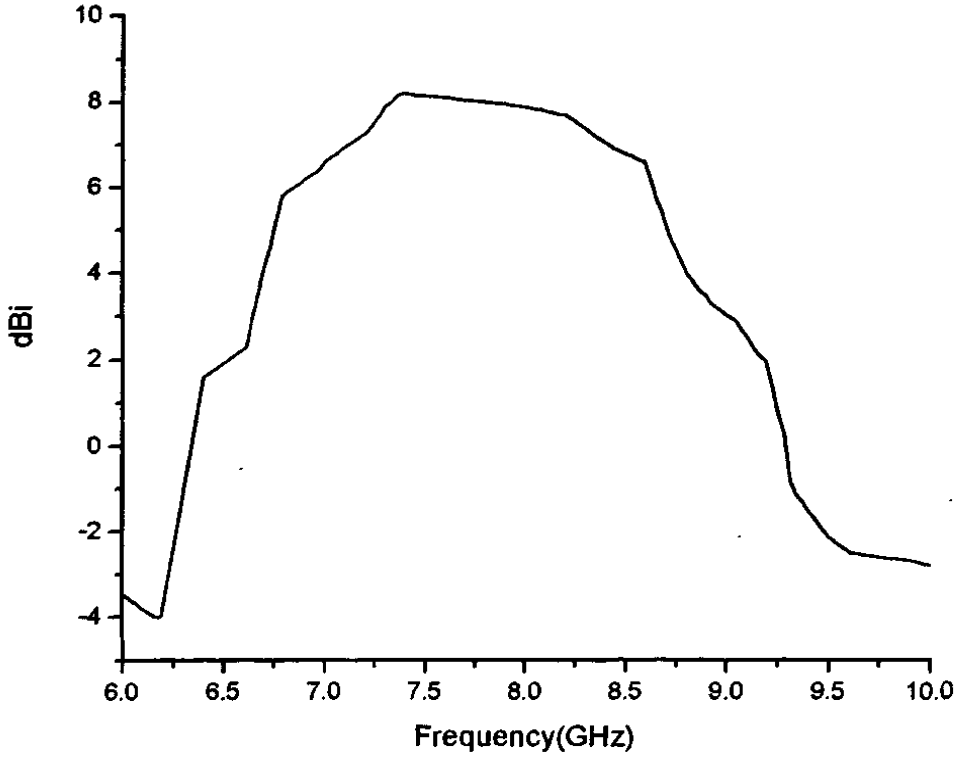

Fig.2.10. Measured antenna gain against frequency.

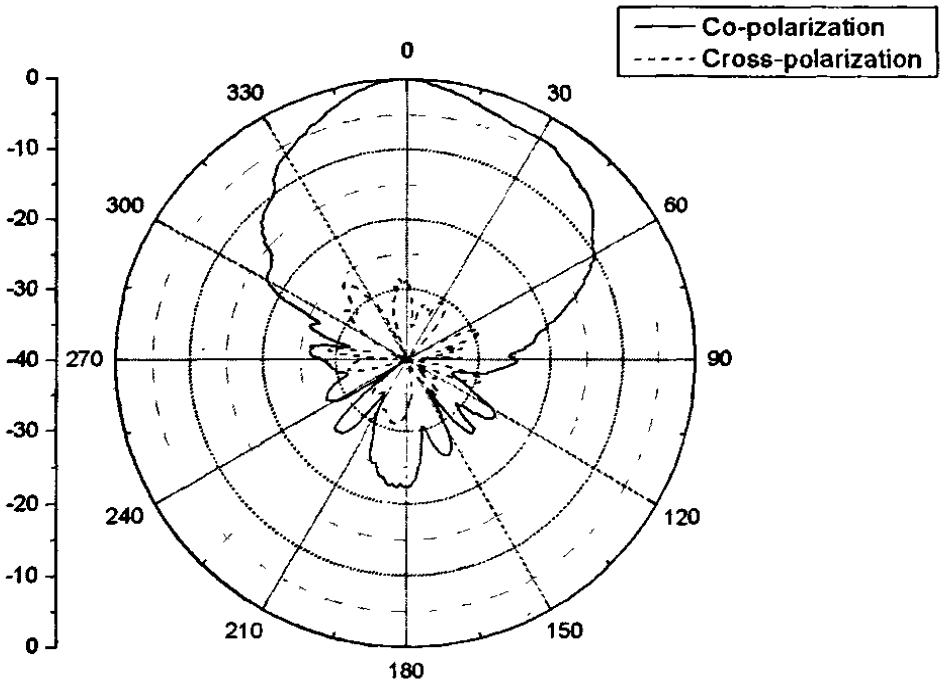

Fig.2.11. Measured radiation patterns (E-plane).

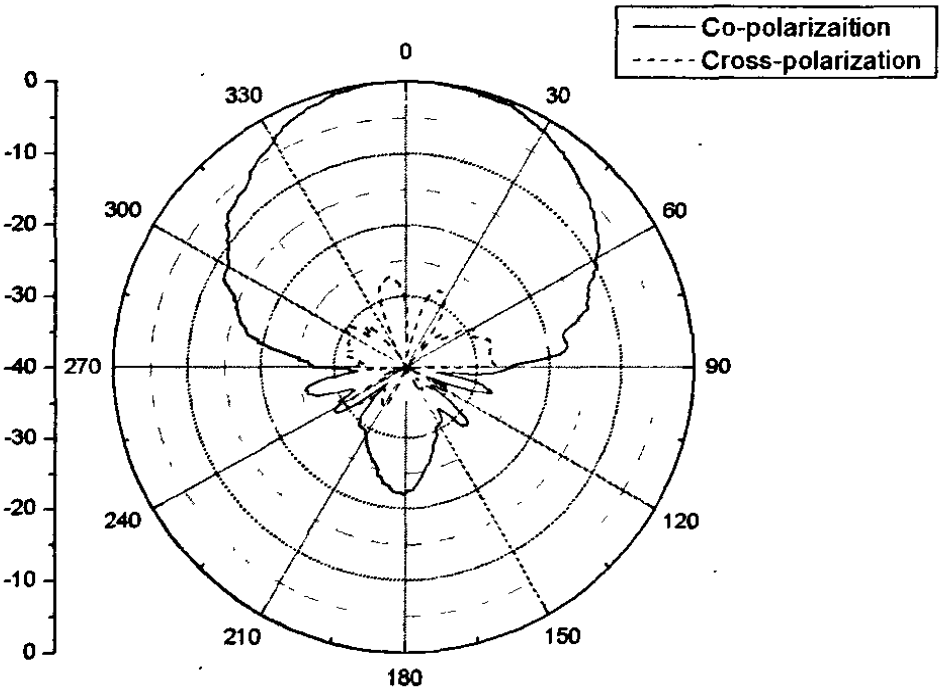

Fig.2.12 Measured radiation patterns (H-plane).

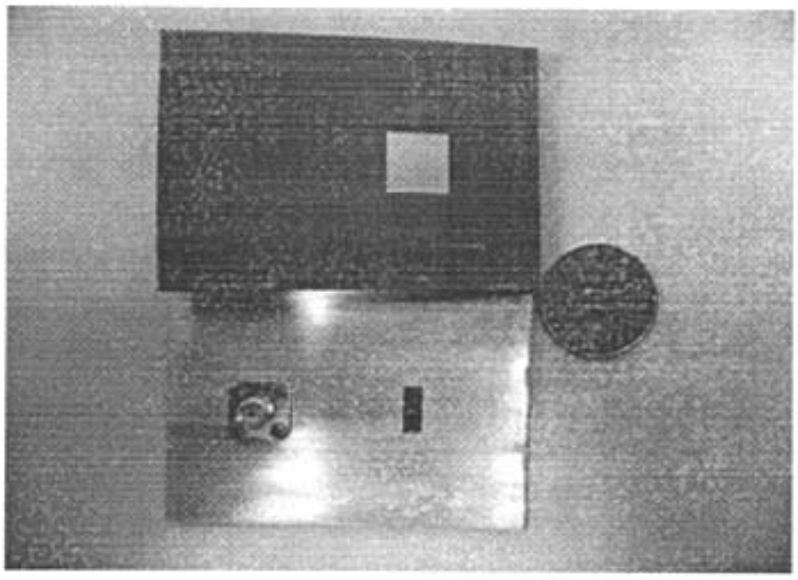

Fig.2.13. Fabricated antenna element (top and bottom views, the feeding structure can not be shown due to the technology of multi-layers PCB).

2.3 Conclusion

A novel fork-like stripline-line fed aperture coupled antenna element is proposed in this chapter. By using the fork-like feeding structure, a broad bandwidth is achieved. The nonresonant aperture is used to suppress the back radiation. The measured E-plane radiation pattern is asymmetric because of the SMA connector at the back of the lower ground plane. This antenna element can be easily expanded into a large array.

3 The Reduction of Mutual Coupling Between Microstrip Antenna Elements

3.1 Literature review

Mutual coupling between the antenna elements in an antenna array is a potential source of performance degradation, particularly in a highly congested environment. Depending on the application, errors due to mutual coupling can be significant. A lot of work has been done to analyze and reduce the mutual coupling between microstrip antennas.

In the case of rectangular patches, extensive studies were carried out for the E and H plane configurations [18]-[20]. In [21], the calculated mutual coupling results for the diagonal and perpendicular orientations are presented and compared with the E and H plane orientations. A numerical analysis of the mutual coupling between two microstrip antennas with coplanar microstrip feed lines is presented in [22]. The impedance matrix and the feed model criteria, which are critical in predicting the input impedance and mutual coupling, are also mentioned and the exact Green's function is used to model a microstrip patch. A detailed description of this microstrip patch model can be found in the literature [23]. A full-wave 3-D FDTD model is used to analyze the mutual coupling between two aperture microstrip patch antennas [24]. The FDTD method solves, in an iterative way, a linearised form of the Maxwell's equations in 3D-space [25].

The coupling coefficients are calculated from the voltages and currents at the input ports of the antenna, rather than from the incident and reflected waves, as is usually done [26]. Use is made of standard two-port network theory, where one port is terminated with a voltage source and its internal resistor and the other port is terminated with a load resistor. The mutual coupling between two electromagnetically coupled three-layer circular microstrip antennas has been investigated experimentally [27]. The measurements have been carried out on the two-element arrays fabricated on different individual substrates for each combination of patch edge spacings.

A full-wave analysis of the mutual coupling between two probe-fed rectangular microstrip antennas on a cylindrical body is presented in [28]. Numerical results of the mutual impedance between antennas and the mutual coupling coefficient S_{21} are calculated using a moment method calculation. The mutual coupling between a pair of Shorted Annular Ring

(SAR) RSW antennas was studied theoretically and experimentally [29]. Reduced Surface Wave (RSW) antennas produce only a small amount of surface wave and lateral-wave radiation since the surface-wave and lateral-wave radiation from the dominant TM01, patch mode is suppressed through proper design [30].

In [31], silicon micromachined structures are utilized as a new efficient microstrip patch antenna. Silicon micromachining process is compatible with current solid state technologies for active circuits. An efficient technique for reducing the coupling is machining the dielectric below the patch, so that there is air below the patch. It is shown that the micromachined substrate can effectively suppress the surface wave excitation and, thus, reduce mutual coupling and increase antenna efficiency. Further, micromachined antennas have wider bandwidth than the conventional patch antenna due to its low effective dielectric constant.

In [31], the radiation along the ground plane is diminished by machining the dielectric under the patch. The radiation is reduced because the polarization currents are removed. Another idea to reduce the horizontal radiation is to compensate the polarization currents by introducing a system of conduction currents that are counter-phased [32]. These new currents are also vertically oriented, so that their magnetic vector-potential cancels out the magnetic vector-potential of the polarization currents. These compensating is introduced by placing shorting posts (pins) between the patch and the ground. The inductive currents in the pins cancel out the capacitive polarization currents. As the result, in a narrow frequency band, the antenna behaves as if there is no dielectric at all.

Some techniques are explicitly designed to suppress the surface wave. In [33] and [34] the antenna dimensions are optimized so that the surface wave is not excited. In [33] the mutual coupling between shorted annular ring reduced surface-wave (SAR-RSW) antennas is investigated and the behavior is compared with conventional circular microstrip patch antennas. The H- and E-plane mutual coupling was significantly less for the SAR-RSW antennas compared to the conventional circular patch antennas for separations greater than a wavelength. The mutual coupling is mainly reduced by virtue of a significant reduction in the space-wave excitation along the interface, at least for thin substrates and moderate patch separations. For larger separations or thicker substrates, the surface wave would become more important, and then a lowering of the mutual coupling would indeed occur through a reduction in the surface-wave excitation. In [34] two variations of a circular microstrip patch design are presented which excite very little surface wave power. Both of the proposed designs are based on the design principle that a ring of magnetic current in a substrate (which models the patches)

will not excite the dominant TM_0 surface wave if the radius of the ring is a particular critical value. The proposed patch designs are chosen to have a radius equal to this critical value, while maintaining resonance at the design frequency. These patch designs excite very little surface wave power, and thus have smoother radiation patterns when mounted on finite-size ground planes, due to reduced surface wave diffraction. These new patch designs also have reduced mutual coupling due to the reduced surface-wave excitation.

Suppression of unwanted surface wave is obtained through making the dielectric be a band-gap structure by printing various patterns on it [35] [36]. Forbidden frequency band for propagation of surface wave can be achieved by periodically loading the substrate. Two different kinds of periodically loaded, grounded dielectric slabs have been investigated. The first kind is realized by drilling holes in the dielectric, while in the second holes are etched in the ground plane. Both kinds of loading may be arranged in a square or triangular lattice.

A novel compact fork-like EBG structure has been investigated [37]. The results verify that the novel EBG structure has a winning feature of compactness. Moreover, this structure provides an additional degree of freedom to control the band-gap characteristics more easily. This feature can be applied to design a wide-band EBG structure. Four columns of fork-like EBG patches are inserted between the E-plane coupled antennas, and the mutual coupling is reduced. A novel dumbbell like 2-D EBG structure is developed in [38]. It has some privileges over the UC-EBG and Patch-via-EBG structures. It is used as an insertion into the space of an E-plane coupled two element array to reduce the mutual coupling between the elements due to surface waves.

Theoretical results and measurements of mutual coupling between active monopoles show that the incorporation of a field effect transistor (FET) with a shunt input inductance leads to large reduction of interactions at reception [39]. Each active monopole then works as an isolated element, and feed requirements of active array become easier to obtain. The performance of receiving monopoles loaded by transistors is studied theoretically as well as experimentally. A knowledge of constant coupling circles enables us to choose appropriate microwave transistors for suppression of mutual effects. On reception, field-effect transistors exhibit interesting parameters; however, a shunt inductance is necessary at the transistor input to obtain the important improvement of mutual coupling. Since mutual coupling effects can be suppressed, design of super-directive array (using active antennas) becomes easier than in the passive case. The required current distribution is adjusted by a correct set of transistor bias and phasing lines.

An effective method to depress mutual coupling between patch antennas by the multi-layer dielectric boards structure is presented in [40]. For simplicity, a patch array antenna with only two probe-fed rectangular patches is dealt with. By adding multi-layer dielectric boards over this original antenna, the modified model is obtained. Both models are simulated obtaining the scattering parameters and mutual impendence. This idea comes from the photonic-band gap (PBG). The thickness of the dielectric boards and the air layers should be modified to obtain a small reflection coefficient and an excellent mutual coupling characteristic. Simulation results indicate that mutual coupling between two patches is greatly depressed when adding multi-layer dielectric boards over the original model.

Metamaterial EM insulators are designed to eliminate mutual coupling between closely packed array elements [41]. For densely packed planar antennas such as rectangular microstrip patch antennas, the mutual coupling between adjacent elements is dominated by trapped waves traveling along the substrate surface. This coupled energy makes input matching and element current excitation control extremely difficult. If mutual coupling can be eliminated, significant improvement in array design may be achievable. Embedded circuit metaMaterials provide highly efficient band-stop rejection. By separating array elements with metamaterial isolation walls, the individual array elements may be designed in isolation without considering mutual coupling- a significant improvement in design and potentially a boon for array designers. In the region around the isolator resonance the isolation wall behaves similar to a perfect magnetic conductor (PMC), providing a reasonably matchable impedance to the nearby patch without the extreme loss effect that a matched absorber would produce when in the near field of a high Q radiating antenna. In fact, near-perfect radiating efficiency is achieved for a single radiating patch surrounded by isolation walls- indicated extremely low isolator wall losses.

The reduction of mutual coupling by using electrically small antenna is studied in [42] [43]. The smaller elements decrease the amount of coupling by increasing the spacing between the elements, thus enhancing the array performance. A linear compact subdivided microstrip square patch array is proposed in [42]. Each subdivided antenna element consists of four comer pads alternating with four high impedance strips attached to a central pad. The subdivided microstrip patch has a 61 % reduction in surface area compared to a conventional square microstrip patch. For the same mutual coupling level as in the conventional patch array, the proposed array can reduce the overall size or insert more array elements in the same board lo obtain enhanced radiation pattern performance. Alternately, the reduced mount of mutual coupling allows one to reduce the size of the array by putting its elements closer. Since the

area of the subdivided microstrip antenna is smaller than that of the conventional microstrip patch antenna, a greater number of antenna elements can be placed in an array within a given area. In the case of a 1D planar array, 1.5n times more subdivided patches can be placed in a given area, where n is the number of conventional elements. If the array was expanded to a 2-D planar array, 2.25n times more subdivided patches can be placed in a given area. Fractal geometries are used to miniaturize the elements [43]. Fractals are geometries developed and defined to mathematically characterize nature. They are generated by repeating an iterative process on a starting structure an infinite number of times. To simulate a fractal geometry as an antenna, only a finite number of iterations can be used. By tightly packing arrays and decreasing mutual coupling using fractal elements, phased arrays may be designed for unique applications with lower scan angles and enhanced performance.

A straightforward way to reduce the mutual coupling of monopole antennas on high-impedance ground plane was developed in [44]. The high-impedance plane (HIP) is a new type of periodic metallic electromagnetic structure that has a band-gap at a fixed frequency. The advantage of this kind of structure results from it having a periodicity much smaller than the free-space wavelength. A thin piece of conducting tape is placed in the middle between the two horizontal monopoles to reduce the mutual coupling, extending throughout the ground plane. This way, destructive interference can be realized by the 180^0 phase shifting caused by the metal strip. The same thought has been adopted in a MIMO microstrip antenna array to reduce the mutual coupling [45]. To suppress mutual coupling, several parasitic elements were employed in the proposed MIMO array antennas. Due to the effect of these parasitic elements, mutual coupling is markedly reduced.

In [45], the reduction of mutual coupling is obtained in a narrow bandwidth (about 3%). This chapter will propose a novel parasitic structure to reduce the mutual coupling through canceling the space wave between the two microstrip patch antennas. The measured results show that the mutual coupling reduction is obtained at 10% bandwidth.

3.2 The reduction of mutual coupling by parasitic structure

3.2.1 Structure configuration

The geometry and the main dimension parameters of the novel parasitic structure

inserted between two microstrip antennas are shown in Fig.3.1. The antennas and the parasitic structure are placed symmetrically about the Y-axis. The two microstrip antennas are fed by two coaxial probes, respectively. The parasitic structure consists of three metal strips along the X-direction, which are connected to each other by a strip along the Y-direction. Two narrow strips are added to the middle X-direction strip, which play the key role in the mutual coupling reduction. The dielectric material used is Arlon DiClad880 with a dielectric constant of 2.2 and a thickness of 1mm.

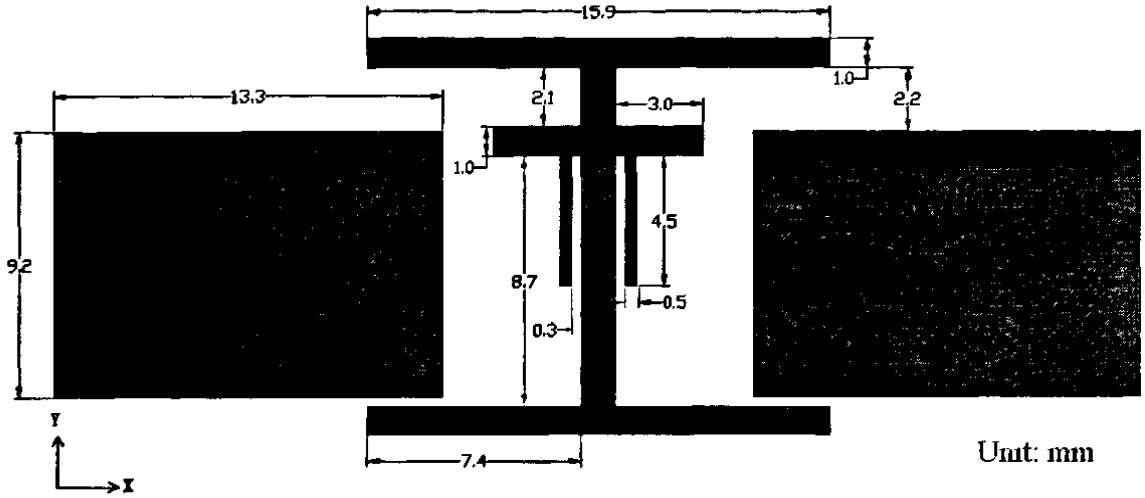

Fig.3.1. The novel parasitic structure inserted between two microstrip antennas

3.2.2 Simulated and measured results

The simulation is performed by the commercial software, Zeland IE3D. The simulated S_{11} and S_{12} parameters are shown in Fig.3.2. The resonant frequency of the patch antennas are 10 GHz. The distance between two normal microstrip antennas is 24mm ($0.8\lambda_{10GHz}$). By adding the novel parasitic structure, the S_{12} parameter is reduced from -27.5dB to -40.7dB at the center frequency, and a 13dB mutual coupling reduction is obtained across a broad bandwidth with only a slight influence on the S_{11} parameter.

The measured S_{11} and S_{12} parameters are shown in Fig.3.3. The measured antenna resonant frequency is 9.75GHz, which is believed to be caused by the fabrication errors. By using the novel parasitic structure, the measured S_{12} parameter is reduced from -26.0dB to -40.6dB at the center frequency, and a 13dB mutual coupling reduction is obtained across a broad bandwidth, which agrees well with the simulated results.

The novel parasitic structure has little influence on the antenna radiation patterns across the 10% bandwidth. As an example, the measured radiation patterns in H-plane and E-plane

at 9.75GHz are shown in Fig3.4. It can be seen that the antenna radiation patterns are little affected. Fig3.5 shows the fabricated structure.

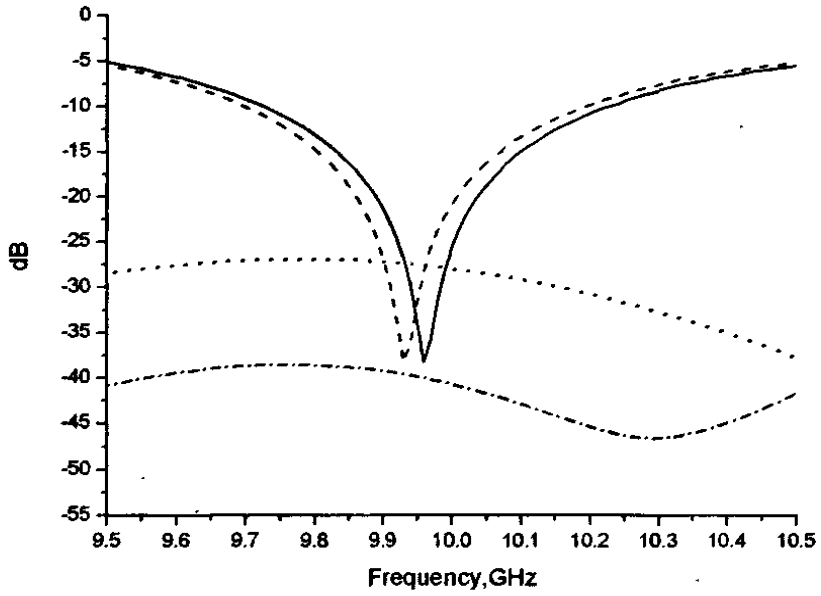

——— simulated S_{11} parameter without the parasitic structure
– – – – simulated S_{11} parameter with the parasitic structure
..... simulated S_{12} parameter without the parasitic structure
–·–·– simulated S_{12} parameter with the parasitic structure

Fig.3.2. Simulated S_{11} and S_{12} parameters.

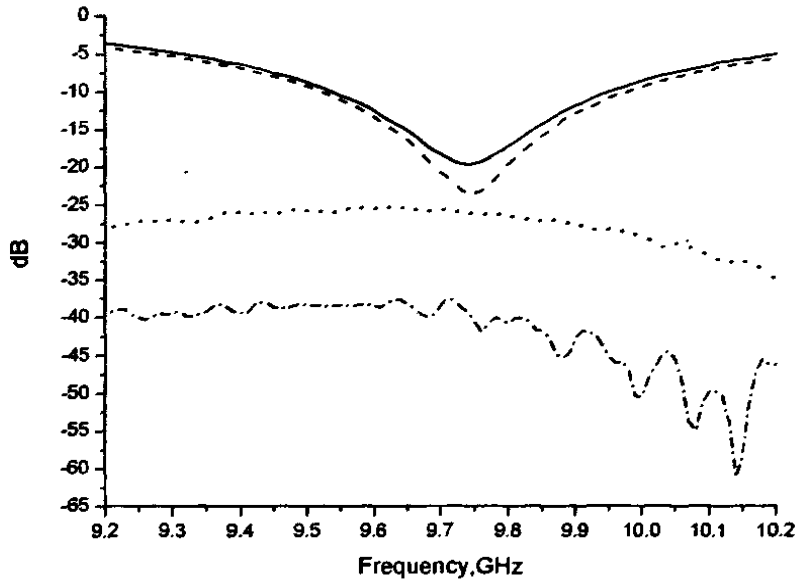

——— measured S_{11} parameter without the parasitic structure
– – – – measured S_{11} parameter with the parasitic structure

..... measured S_{12} parameter without the parasitic structure
——— measured S_{12} parameter with the parasitic structure

Fig.3.3. Measured S_{11} and S_{12} parameters.

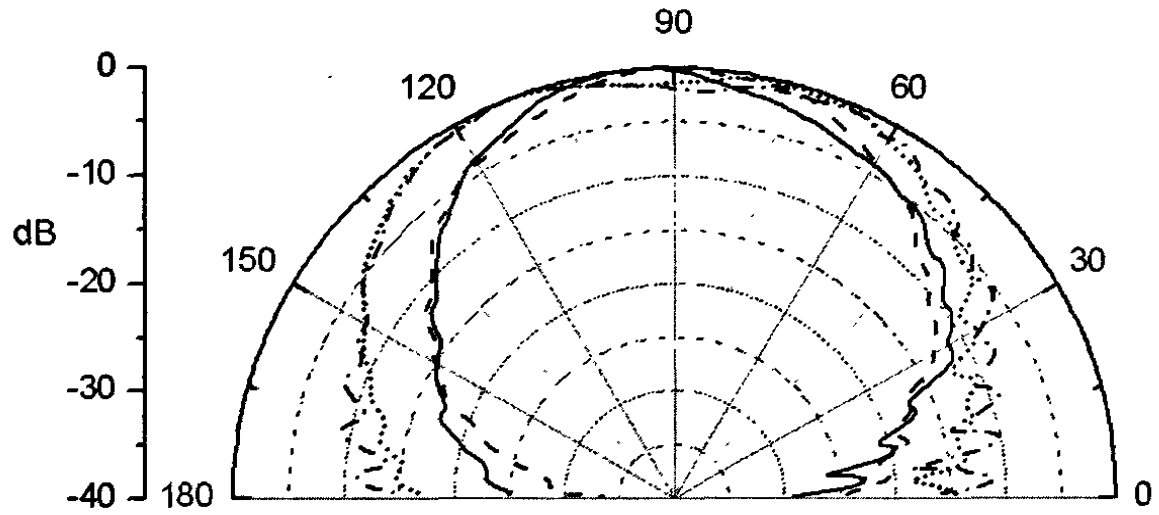

——— measured H-plane radiation pattern without the parasitic structure
– – – – measured H-plane radiation pattern with the parasitic structure
.....measured E-plane radiation pattern without the parasitic structure
–·–·–·– measured E-plane radiation pattern with the parasitic structure

Fig.3.4. Measured H-plane and E-plane radiation patterns at central frequency.

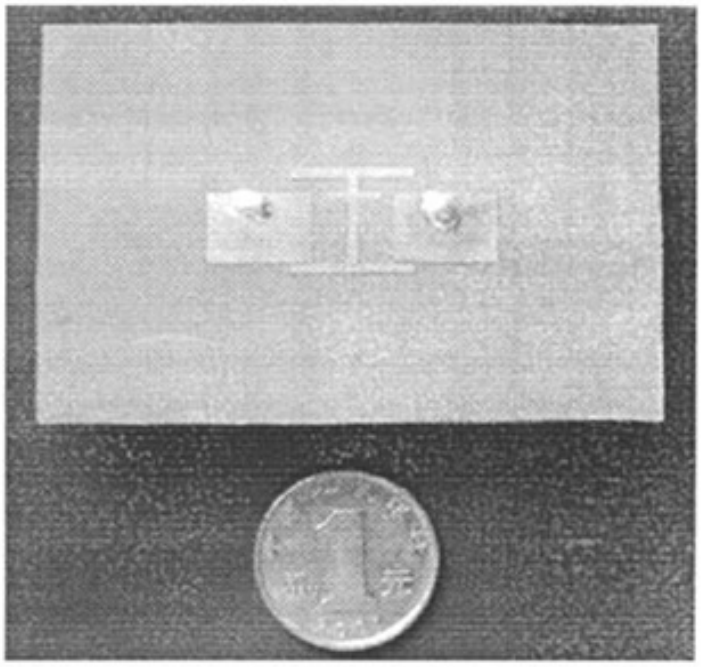

Fig.3.5. Fabricated antennas with parasitic structure.

3.3 Conclusion

In this chapter, the mutual coupling between two microstrip antennas is reduced by implementing a novel parasitic structure. The measured results show a 13dB mutual coupling reduction across 10% bandwidth without affecting the radiation patterns. This structure can be easily integrated into an adaptive antenna array to improve the null depth, or into a MIMO system to achieve a good isolation between antenna elements.

4 The Calculation and Reduction of Mutual Coupling Between Microstrip Antenna Arrays

4.1 Mutual impedance formula based on synthetic asymptote and variable separation

4.1.1 Theory

The impedance formula is introduced here for completeness [46]. Like the Green's function of a point source, the mutual impedance between two antenna elements as extended sources can still be divided into three regions in terms of the center-to-center separation r between the elements, say patches, in Fig. 4.1. That is:

a) The near field for closely spaced adjacent patches with a static dependence of $1/r^{n+1}$, where $n \geq 1$, this forms the near asymptote of r ;

b) The far field for widely separated patches, with a spherical wave dependence of $1/r$, this forms the far asymptote ;

c) The surface wave zone for even wider separation with a cylindrical wave dependence of $1/r^{1/2}$, this forms the "far-far" asymptote that may sometimes be neglected - the reason is that the surface wave may become significant only at $10\lambda_0$ or beyond, this distance could be outside the finite boundary of the antenna array.

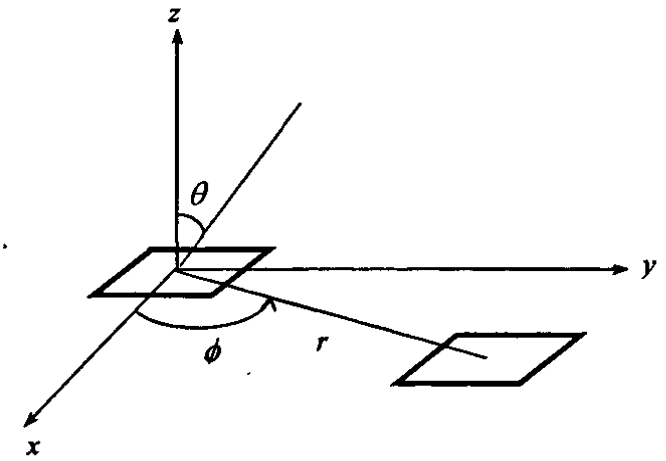

Fig. 4.1. Coordinates of two coupling patches in an array.

Taking advantage of the knowledge of static variable separation in near field, radiation pattern in far field, and the possible combination of them two by synthetic asymptote, it is found that the mutual impedance between two arbitrary elements can be written in a generalized form of separated variables. In principle, there are four significant terms in $1/r^{n+1}$ with n = -1/2, 0, 1 and 2 for the far asymptotic couplings of surface wave and radiation, and the near asymptotic couplings of static dipole and quadrupole. Three Fourier components of the azimuth angle ϕ with the symmetry relations are used, that is: constant, $\cos 2\phi$ and $\cos 4\phi$. Thus, by the simple sum of synthetic asymptote, the mutual impedance between two elements can be written in a series with the unknown complex coefficients $C_{n,m}$ as

$$Z_{ab} = \eta_0 \frac{e^{-jk_0 r}}{4\pi} \sum_{n=-1/2,0,1,2} \{[1/(k_0 r)^{n+1}] \times [C_{n,0} + C_{n,2}\cos(2\phi) + C_{n,4}\cos(4\phi)]\} \qquad (4.1)$$

where η_0 is the intrinsic impedance of free space. The 12 unknown coefficients $C_{n,m}$ in formula (4.1) can be found by matching with numerical solutions, or measured values, between the center patch "0" and the 12 coupling patches in a skeleton array as shown in Fig. 4.2. The boundary of the skeleton array may correspond to the boundary of an actual array to be analyzed. Evidently with this sampling principle, the intermediate patches within the boundary may be selected arbitrarily without significantly increasing the error in the resulted formula of (4.1).

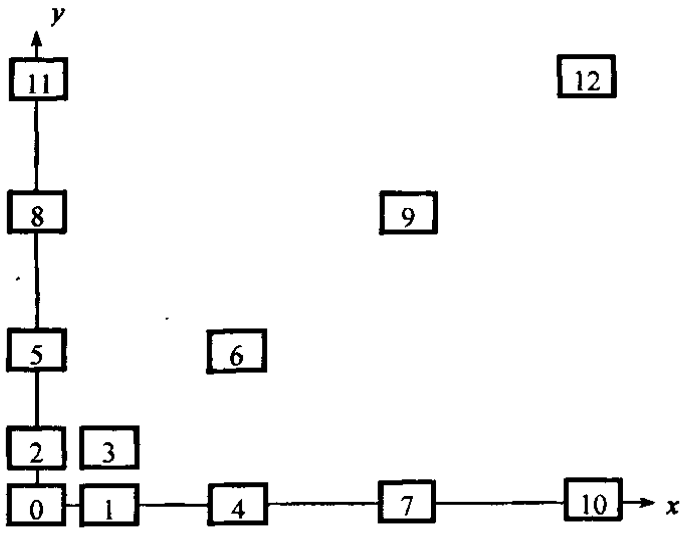

Fig. 4.2. The layout of sampled mutual couplings between the zeroth patch and the *nth* patch (n = 1 to 12) for evaluation of the 12 $C_{n,m}$ coefficients.

The generalized form of separated variables in (4.1) is obtained from its novel physical

base. Being more complete and general, it should be more accurate than other formula for mutual coupling including Bailey's formula [47]. It is emphasized that, with appropriate sampling, this formula incorporates the current distortion on the two closely spaced elements. Thus it can still give the accurate result in this case. Furthermore, this formula has the advantages of high efficiency, with no restriction on the detailed structures of element, feed and substrate.

4.1.2 The selection of full wave solver

The mutual impedances terms Z_{ab} between two isolated patches can be calculated by the closed form formula (4.1). The 12 unknown coefficients $C_{n,m}$ in formula (4.1) can be found by matching with numerical solutions obtained from full wave solver.

Consider two kinds of popular commercial software: Zeland IE3D and Ansoft Designer, which are both based on MoM. Fig.4.3 shows the layout of an aperture coupled microstrip antenna. The radiating patch is etched on a substrate layer with thickness h_1=0.5mm and ε_r=2.7. A 2mm-thick air spacer is inserted between the substrate layer and the ground plane to get a good return loss. A coupling aperture is etched in the ground plane. The microstrip feed-line is etch on a substrate layer with thickness h_1=0.5mm and ε_r=2.7. The center frequency of this antenna is 10GHz.

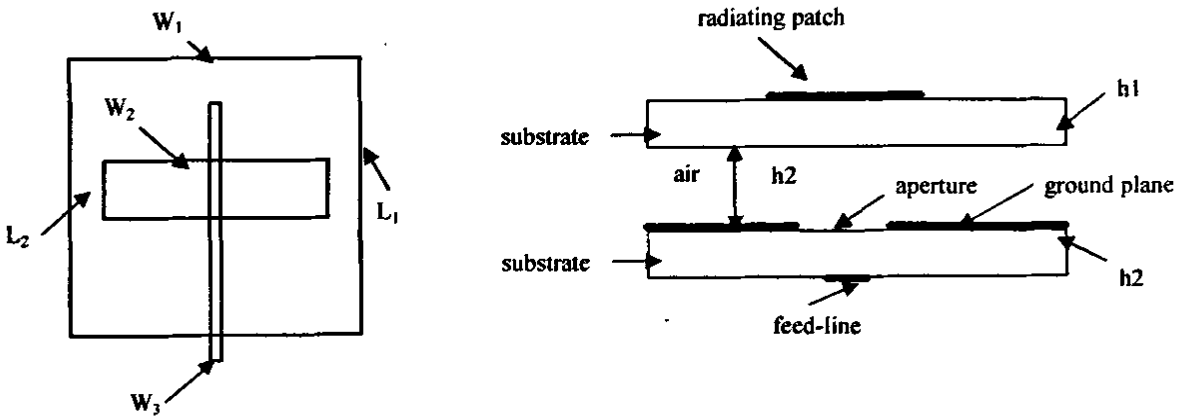

(a) Geometry of the antenna (b) Cross-sectional view

Fig. 4.3. The layout of an aperture coupled microstrip antenna.
W_1=9.2mm, L_1=9.1mm, W_2=7.2mm, L_2=1.9mm, W_3=0.4mm, h_1=0.5mm, h_2=2mm

Fig.4.4 shows the mutual coupling parameter S_{21} versus spacing for two identical antennas. The antenna is the same as the one depicted in Fig.4.3. The parameter d is the spacing between the two antennas. It can be seen that the results of IE3d match well with those

of Ansoft Designer when spacing d is less than $2\lambda_0$. As the spacing d becomes larger, the mutual coupling parameter S_{21} becomes smaller. It can be seen in Fig.4.7 that when the two antennas are H-plane coupled, the calculated results of IE3D oscillate between -55dB and -60dB in case spacing d is larger than $5\lambda_0$. But the curve of Ansoft Designer is still smooth. So Ansoft Designer is used in the next section to calculate the numerical solutions which are needed to find the 12 unknown coefficients $C_{n,m}$ in formula (4.1).

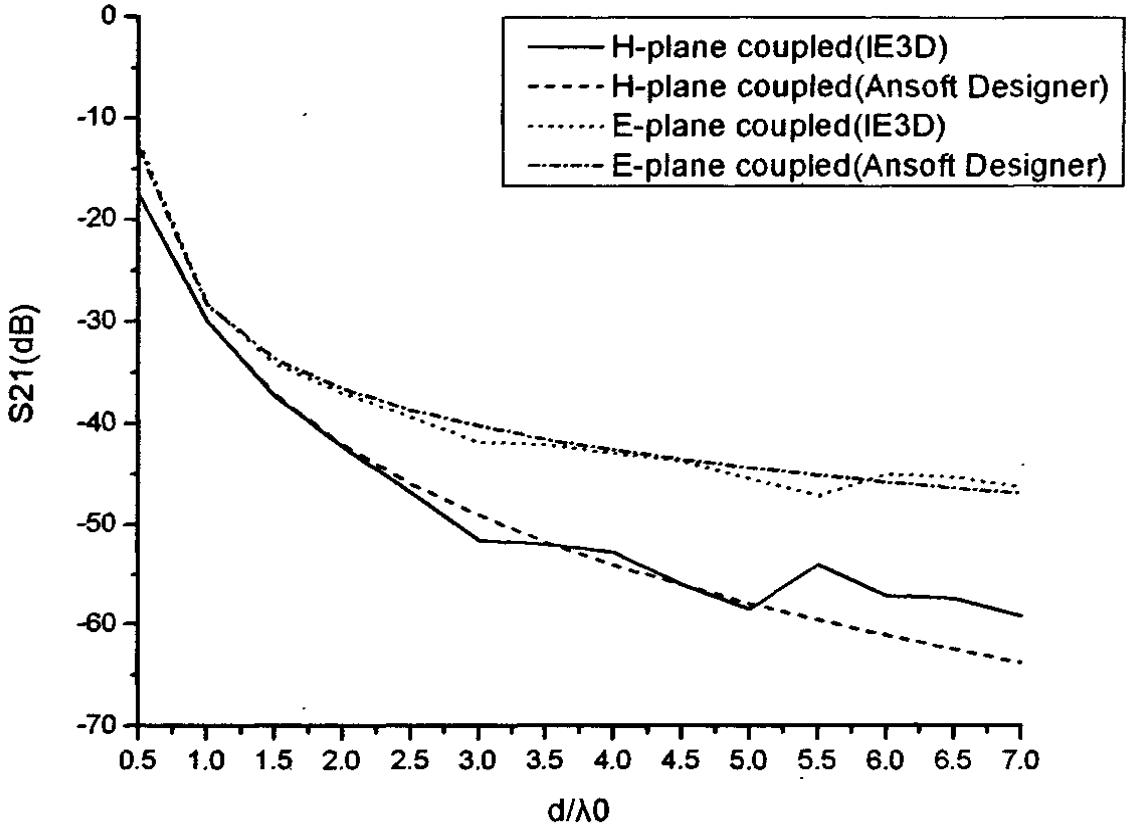

Fig.4.4. Mutual coupling parameter versus spacing for two H-plane coupled antennas

4.1.3 The extrapolation characteristic

There are 12 unknown coefficients $C_{n,m}$ in formula (4.1), which means 12 samples of the isolated mutual impedance *Zab* are needed to find these unknown coefficients. Consider the 64 radiating elements of an 8*8 antenna array, as is depicted in Fig.4.5. The antenna element is the same as the one depicted in Fig.4.3. The antenna element spacing is d along both H-plane and E-plane. The spacing d is set to be 24mm ($0.8\lambda_0$) to obtain the maximum

gain [48]. The center element in Fig.4.5 is set to be at the position (0mm, 0mm). The positions of the 12 sample elements are also shown in Fig.4.5. Then the isolated mutual impedance Z_{ab} is calculated between the center element and each sample element to obtain the unknown coefficients $C_{n,m}$. Once the 12 unknown coefficients $C_{n,m}$ are found, the isolated mutual impedance between every two elements of the array can be given by formula (4.1).

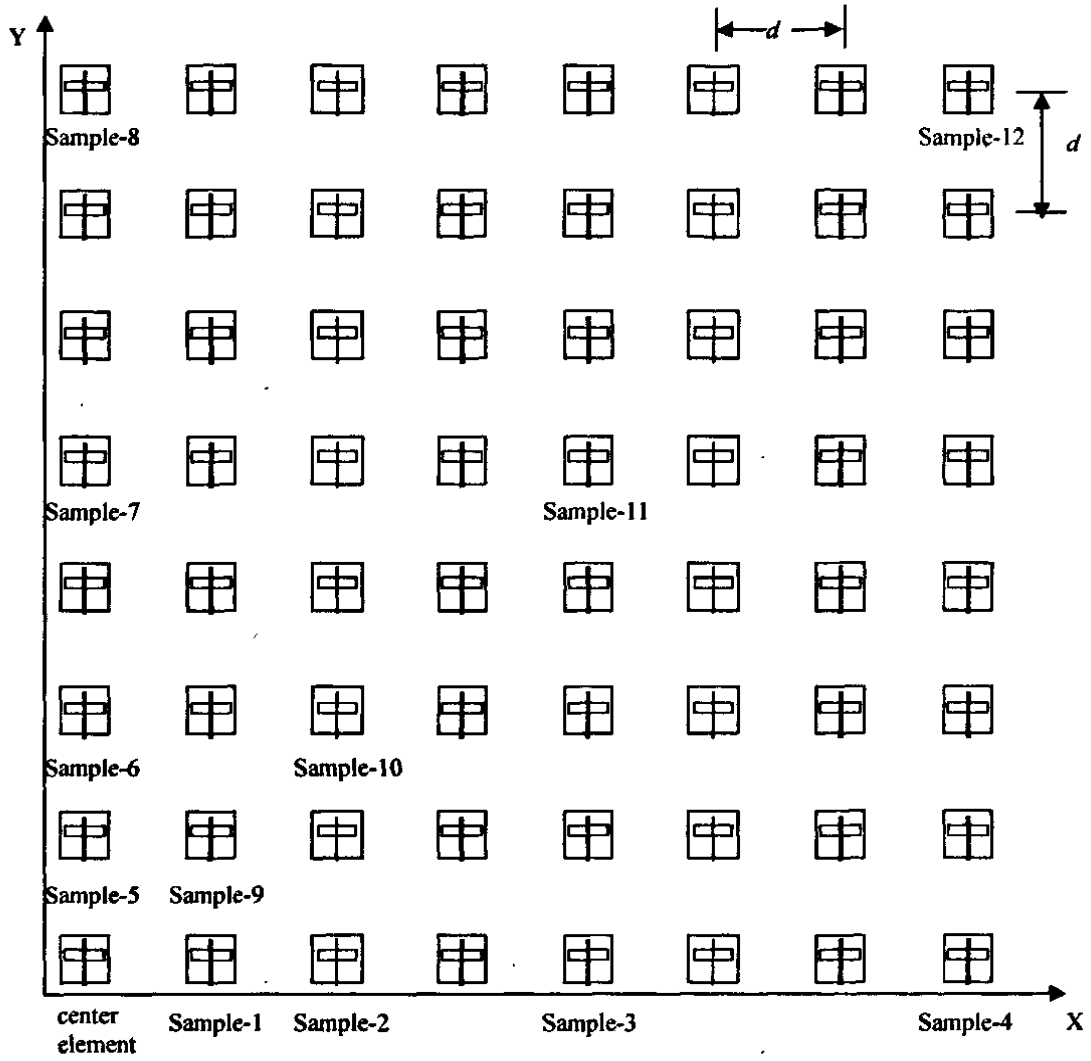

Fig.4.5. The 12 samples of Z_{ab} for evaluation of the 12 $C_{n,m}$ coefficients.

Consider the calculation of mutual coupling between two 8*8 aperture coupled antenna arrays by network method. The two arrays are H-plane coupled and the spacing between the centers of the two arrays is 192mm ($6.4\lambda_0$). In this situation there are totally 128 radiating elements. The element located at the 1st column and 8th row is set to be the center element, and it is placed at the coordinate of (0, 0). Formula (4.1) is used to calculate the isolated mutual impedance between the center element and the rest 127 elements. The positions of the 12 sample elements for evaluation of $C_{n,m}$ are the same as depicted in Fig.4.5. The thirteen-element array composed of the center element and the 12 sample elements is called

the skeleton array. 64 elements are inside the skeleton array (from column 1 to column 8), while 64 elements are outside of the skeleton array (from column 9 to column 16). As is shown in [46], formula (4.1) can accurately calculate the isolated mutual impedance between the center element and elements inside the skeleton array. But when formula (4.1) is extrapolated to calculate the isolated mutual impedance between the center element and elements outside of the skeleton array, the accuracy need to be checked out.

Table 4.1 shows the comparison of the isolated mutual impedances given by formula (4.1) and those calculated by Ansoft Designer for elements outside of the skeleton array. The mutual impedance Z_{ab} is calculated between the center element and the second element, and the coordinate of the second element is given in Table.4.1. It can be seen that these two results agree well with each other. Formula (4.1) has a good extrapolation characteristic, and can be used to accurately calculate the isolated mutual impedance between the center element and the rest 127 elements.

Table.4.1. The comparison of the isolated mutual impedance given by formula (4.1) and that calculated by Ansoft Designer (for elements outside of the skeleton array).

Out of the skeleton array					
Coordinate (mm)	Z_{ab} (by formula)	Z_{ab} (by Ansoft Designer)	Coordinate (mm)	Z_{ab} (by formula)	Z_{ab} (by Ansoft Designer)
(264, 0)	-0.0526-0.0602i	-0.0541-0.0590i	(264,96)	0.1226-0.0041i	0.1242-0.0039i
(336, 0)	0.0040+0.0486i	0.0071+0.0487i	(312,96)	-0.0843+0.0113i	-0.0858+0.0122i
(0, 264)	-0.7264+0.0459i	-0.7281+0.0532i	(360,96)	0.0576-0.0218i	0.0586-0.0238i
(0, 336)	0.5281+0.2829i	0.5374+0.2719i	(216,144)	-0.1194-0.2214i	-0.1183-0.2232i
(72, 264)	0.3221+0.5717i	0.3341+0.5653i	(264,144)	-0.0534+0.1628i	-0.0546+0.1634i
(144,336)	0.3949+0.2557i	0.4035+0.2413i	(360,144)	-0.0714+0.0523i	-0.0719+0.0535i
(240,24)	-0.0760+0.0647i	-0.0756+0.0660i	(216,168)	0.0995+0.2625i	0.0984+0.2635i
(288,24)	0.0192-0.0660i	0.0175-0.0672i	(264,168)	0.1450-0.1325i	0.1458-0.1321i
(360,24)	-0.0355+0.0245i	-0.0343+0.0275i	(360,168)	0.0950+0.0436i	0.0958+0.0432i
(216,48)	0.1337+0.0256i	0.1349+0.0256i	(336,48)	0.0440+0.0307i	0.0464+0.0293i

4.2 The in-array impedance formula

The formula for mutual coupling is very accurate compared with full wave analysis, e.g. IE3D, based on the assumption that the patches concerned are in isolation without other nearby patches. This gives, of course, a first approximation of the array impedance matrix which we called isolated impedance matrix $[Z^{iso}]$ because all the parasitic elements are ignored. Jackson *et al.* [49] have proposed a correcting procedure which only needs the knowledge of the isolated element input impedance and mutual impedance of two isolated elements, finally leading to a corrected matrix $[Z^{inar}]$, i.e. the in-array impedance matrix, which is a good approximation of the real one. Because this procedure makes use of the surface mode currents on the patches to calculate the mutual coupling effects, the current induced on the parasitic elements can be naturally involved. The primary relations are presented as following:

Consider patch m in an N patch array, let v_m be the dominant mode voltage produced by a unit amplitude current mode. Then the port voltage V_m is

$$V_m = a_m v_m + jI_m X_{fm} \tag{4.2}$$

where I_m is feed current, X_{fm} is the feed reactance of patch m; the dominant mode current amplitude on the mth patch may be written as

$$a_m = e_m I_m + \sum_{n \neq m} a_n M_{mn} \tag{4.3}$$

where M_{mn} is the mutual coupling coefficients between element m and n, provided the assumption is made that only the dominant modes contribute to the coupling. e_m is the excitation coefficient. According to the definition of impedance matrix, the corrected matrix $[Z^{inar}]$ can be obtained through a series of matrix manipulation

$$[Z^{inar}] = [v]([U] - [M])^{-1}[e] + j[X_f] \tag{4.4}$$

with $[U]$ the identity matrix and $[v],[e],[X_f]$ the diagonal matrices of dimension $N \times N$. In the case of identical patches and feeds

$$[e] = e[U], [v] = v[U], [X_f] = X_f[U],$$

then (4.4) reduces to

$$[Z^{mar}] = Z_S^{iso}([U]-[M])^{-1} + jX_f[U] \tag{4.5}$$

where Z_S^{iso} is the "subtracted" input impedance of an isolated patch—the total input impedance minus the feed reactance; $[M]$ is the mutual coupling coefficient matrix. The terms M_{mn} can be determined by relating to the isolated mutual impedance Z_{mn}^{iso} (i.e. Z_{ab} of (4.1)) in the following form

$$Z_{mn}^{iso} = \frac{v_m e_n M_{mn}}{1 - M_{mn} M_{nm}} \tag{4.6}$$

Assuming identically shaped patches ($M_{mn} = M_{nm}$) and identical feeds ($e_m = e_n$), $[M]$ can be solved by:

$$M_{mn} = \frac{1}{2Z_{mn}^{iso}}[-Z_S^{iso} + ((Z_S^{iso})^2 + 4(Z_{mn}^{iso})^2)^{1/2}] \quad \text{for } m \neq n \tag{4.7}$$

$$M_{mn} = 0, \qquad \text{for } m = n \tag{4.8}$$

If the row and column norms of $[M]$ are less than one in magnitude, i.e. the coupling is sufficiently weak, the following expansion for terms in (4.5) may be used to avoid the matrix inversion,

$$([U]-[M])^{-1} = [U] + [M] + [M]^2 + \cdots \tag{4.9}$$

Fortunately, formula for the self-impedance of isolated patch is available [50], [51]. And the mutual impedances terms $Z_{mn}^{iso}(m \neq n)$ between two isolated patches can be calculated by the closed form formula in instead of using the moment method, which can vastly reduce the computer time, making the Jackson's procedure more efficient in analyzing the finite array. The reason lies in that the time consumed in calculating formula (4.1) can almost be neglected, compared with carrying the MoM for calculating each pair of $Z_{mn}^{iso}(m \neq n)$. As a result, the larger the array is, the more time can be saved. The only limitation comes from the assumption of the Jackson's procedure that the elements are characterized by a single radiation mode. However, this assumption will not lead to the unacceptable errors, because microstrip patch is a highly resonant structure, and near the resonance its current distribution can be well approximated by a single mode. This distribution is not greatly affected by the proximity of nearby elements in an array (assuming the elements are not too closely spaced) [51].

Finally, the scattering matrix (for identical patch shapes and feeds) may be found from

subsititution of (4.5) into the classical formula, that is

$$[S] = ([Z^{inar}](1/[Z_0]) - [U])([Z^{inar}](1/[Z_0]) + [U])^{-1} \tag{4.10}$$

with Z_0 the feed line impedance.

4.3 The calculation of mutual coupling between antenna arrays using network method

Fig.4.6 shows the main procedure of the calculation of the mutual coupling between two 8*8 microstrip antenna arrays by network method. The two arrays are separated into two parts: the 128 radiating elements and the feeding networks, as is shown in Fig.4.7 and Fig.4.8, separately.

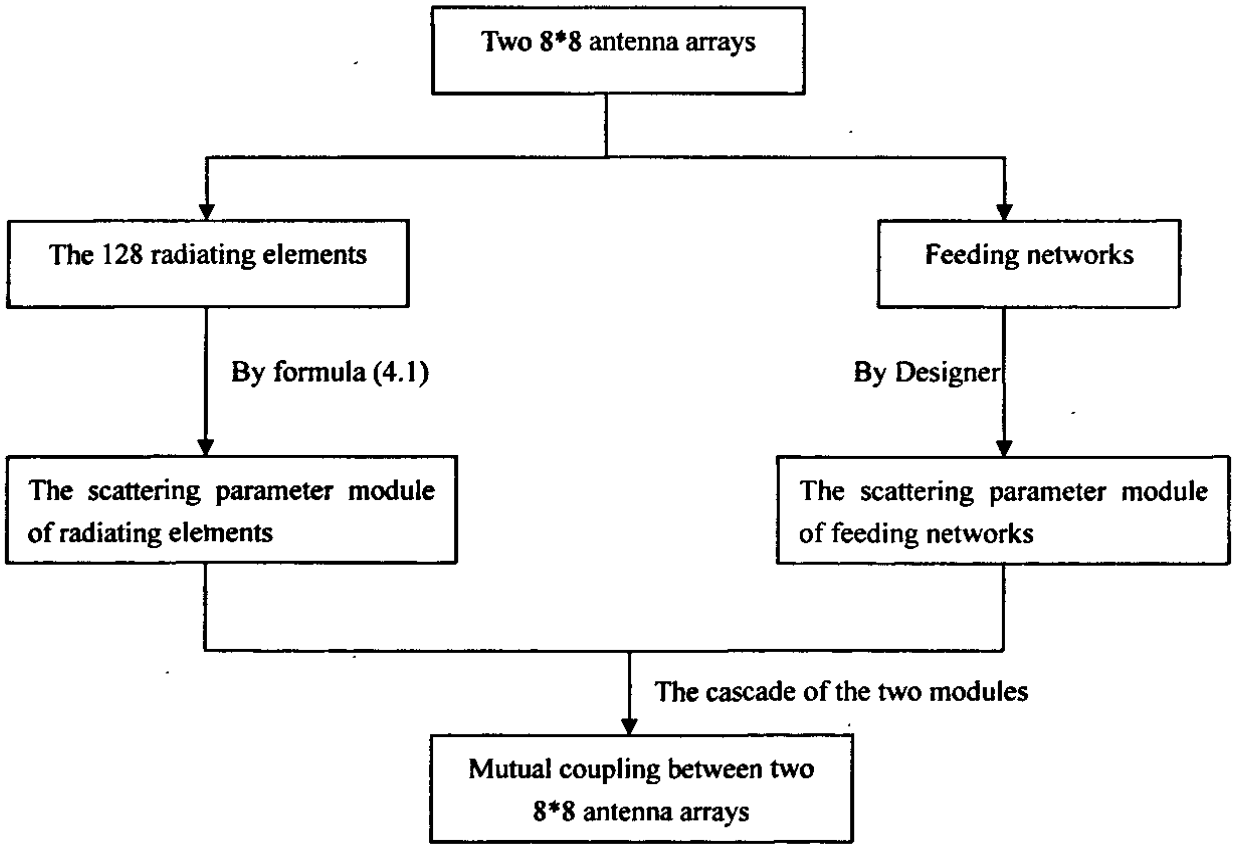

Fig.4.6. The main procedure of the calculation of the mutual coupling between two 8*8 microstrip antenna arrays by network method.

As is shown in Section 4.1.3, formula (4.1) can be used to accurately calculate the isolated mutual impedance between the center element and the rest 127 elements in Fig.4.7. Then the 128*128 matrix Z_S^{iso} in formula (4.5) is easy to be obtained. The matrix $[M]$ in

formula (4.5) is obtained from formula (4.7) and (4.8), while $[X_f]$ equals to zero. So the corrected matrix $[Z^{mar}]$ can be calculated by formula (4.5). The scattering parameters of the 128 radiating elements are then given by formula (4.10), while that of the feeding networks is calculated by Ansoft Designer. Then the two parts are loaded as two parameter modules, which are cascaded to obtain the mutual coupling parameter S_{21}.

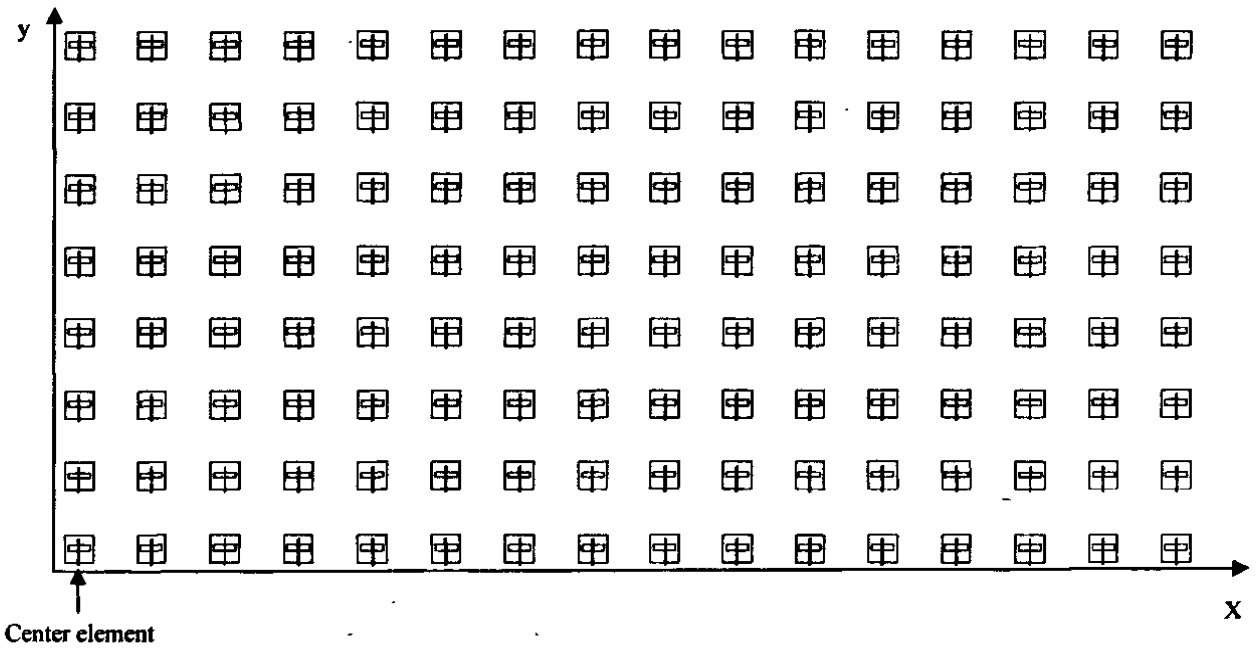

Fig.4.7. The layout of 128 radiating elements.

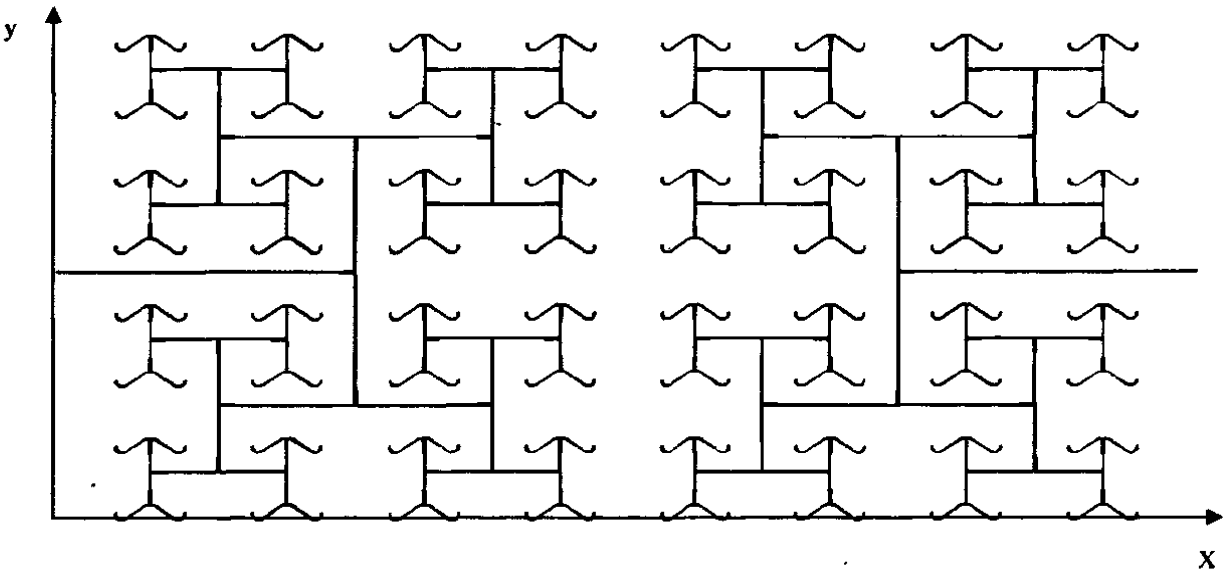

Fig.4.8. The layout of the feeding network

Table 4.2 shows the comparison between results obtained from full wave analysis of the whole arrays and those from the network method. It can be seen that the calculated results of Ansoft Designer agrees well with those of the network method at center frequency 10GHz.

The computation time is reduced from 180 minutes to 30 minutes on a personal computer (CPU: P4/2.0G; memory: 1.0G).

Errors are observed when using the loading method to calculate the mutual coupling between two microstrip antenna arrays composed of elements fed by coplanar microstrip lines. This is because in this situation the feeding networks lie in the same layer as the radiating elements, and the spurious radiation from the feed lines affects the mutual impedance of the radiating elements.

Table.4.2. The comparison of calculated results between full wave analysis and network method

Frequency=10GHz	S_{11}(dB)	S_{12}(dB)	Computation time
Ansoft Designer	-14.1	-47.5	180 minutes
network method	-14.4	-48.4	30 minutes

4.4 The reduction of mutual coupling between antenna arrays through adjusting the element spacing

For a radar using continuous wave, when the scheme of twin antennas is used, the transmitting antenna array and the receiving antenna array will be closely placed side by side. If the mutual coupling is too strong, the transmitting energy will blockade the receiver. Therefore the reduction of mutual coupling between two arrays is very important. The polarization isolation and frequency isolation are fundamental measures to reduce the mutual coupling, however they are not available in case of the requirements of the same polarization and frequency band of two arrays.

I did not find any report on the mutual coupling reduction between two arrays except Mailloux's paper [52]. In that paper, a theoretical and experimental study are presented on the use of thin perfectly conducting fence to reduce the mutual coupling of two parallel-plane waveguides radiating through a ground plane.

The two 8*8 array designed in the last section have a mutual coupling of -47.5dB. In this section, the element spacing d in the H-plane (the plane along x-direction) is adjusted to reduce the mutual coupling between two 8*8 aperture coupled antenna arrays. The element spacing in the E-plane is fixed at 24mm ($0.8\lambda_0$). The spacing between the centers of two 8*8 arrays is fixed at 192mm ($6.4\lambda_0$).

The required performances of the antenna array are shown as follows:

•Center frequency: 10GHz

•Bandwidth: 10% (VSWR<2)

•Polarization: linear

•Side lobe levels (SLLs): <-12.5dB

•The gain across the bandwidth: >23dB

•The mutual coupling between two arrays: <-55dB

When doing the adjustment, only the scattering parameters of the feeding network need to be calculated by Ansoft Designer for different element spacings, and the scattering parameters of the radiating elements are given by formula (4.10). The time consumed for the calculation of mutual coupling for each element spacing d is reduced from 180 minutes by Ansoft Designer to about 30 minutes by network method.

4.4.1 The formulas for calculating radiation pattern and directivity based on array factor

The change of element spacing will cause the change of radiation pattern, directivity and return loss. All these factors need to be considered when designing antennas with a good performance. The formulas for calculating radiation pattern and directivity based on array factor are illustrated in [53].

The pattern of a rectangular array is the product of the array factors of the arrays in the x- and y-directions. The normalized array factor for the entire planar array can be written as:

$$AF = S_{xm} S_{yn} \tag{4.11}$$

Where S_{xm} is the array factor in the x-direction; S_{yn} is the array factor in the y-direction. Here m=n=8, and the antenna elements are equally placed in the x-direction with spacing d_x and in the y-direction with spacing d_y.

So S_{xm} and S_{yn} in formula (4.11) may be written as

$$S_{xm} = \sum_{n=1}^{M} e^{i(m-1)kd_x \sin\theta\cos\phi} \tag{4.12}$$

$$S_{yn} = \sum_{n=1}^{N} e^{i(n-1)kd_y \sin\theta\sin\phi} \tag{4.13}$$

Because the element spacing is not changed along the y-direction during the optimization, only the radiation pattern variation along the x-direction (H-plane) need to de evaluated for brevity. So in formula (4.12) and (4.13) the variable Φ is set to be 0^0 when calculating the H-plane radiation pattern. Then the normalized array factor can be reduced to

$$AF = S_{xm} = \sum_{n=1}^{M} e^{j(m-1)kd_x \sin\theta} \tag{4.14}$$

and the radiation pattern can be plotted by the following formula

$$R(\theta) = 20\log_{10}(|\mathrm{AF}(\theta)|/|\mathrm{AF}(\theta)|_{\max}) \tag{4.15}$$

where θ varies from -90^0 to 90^0.

The directivity of array factor $AF(\theta,\Phi)$ whose major beam is pointing in the $\theta=\theta_0$ and $\Phi=\Phi_0$ direction, can be written as:

$$D_0 = \frac{4\pi[AF(\theta_0,\phi_0)][AF(\theta_0,\phi_0)]^*|_{\max}}{\int_0^{2\pi}\int_0^{\pi}[AF(\theta,\phi)][AF(\theta,\phi)]^* \sin\theta d\theta d\phi} \tag{4.16}$$

For large arrays, which are nearly broadside, the directivity reduces to

$$D_0 = \pi \cos\theta_0 D_x D_y \tag{4.17}$$

and

$$D_0(dB) = 10\log_{10}(\pi\cos\theta_0) + 10\log_{10}(D_x) + 10\log_{10}(D_y) \tag{4.18}$$

where D_x and D_y are the directivities of broadside linear arrays each, respectively, of length and number of elements L_x, M and L_y, N. The factor $\cos\theta_0$ accounts for the decrease of the directivity because of the decrease of the projected area of the array. Here θ_0 equals to zero because the radiating elements are fed with the same amplitude and phase.

In formula (4.18), D_y is not changed because the element spacing is not changed along y-direction, so the variation of D_x gives an accurate approximation to the variation of D_0. D_x can be calculated by formula (4.16). AF(θ,Φ) in formula (4.16) is given by formula (4.14), and θ_0 equals to zero.

4.4.2 Reduction of mutual coupling

Fig.4.9 shows the S_{21} parameters between two 8*8 antenna arrays calculated by network method for different spacing d/λ_0. The S_{21} parameters calculated by Ansoft Designer are also presented for comparison. As is expected, the two results agree well with each other. The maximum error is 3dB at d/λ_0=0.7. The total calculation time is much less by network method than by Ansoft Designer. It is seen that the minimum mutual coupling occurs at d/λ_0 =0.57 and 0.7, respectively. Compared with the mutual coupling level between two arrays designed in Fig 4.5 (d/λ_0=0.8), a 10dB reduction of mutual coupling is obtained at d/λ_0=0.57 and 0.7, respectively, and the mutual coupling between two arrays is less than -55dB at these two kinds of spacing.

Table 4.3 shows the calculated variation of directivity for different element spacing d/λ_0. ΔD is given by the following formula

$$\Delta D = D_s - D_{d/\lambda 0=0.8} \tag{4.19}$$

Where D_s is the directivity of an 8*8 array with a given element spacing d, and $D_{d/\lambda 0=0.8}$ is the directivity of an 8*8 array with spacing d/λ_0 =0.8. Both D_s and $D_{d/\lambda 0=0.8}$ are given by formula (4.18). Then ΔD can be reduced to

$$\Delta D(dB) = 10\log_{10}(D_{x,s} / D_{x,d/\lambda 0=0.8}) \tag{4.20}$$

Where $D_{x,s}$ is the directivity of a 1*8 subarray along x-direction with a given spacing d, and $D_{x,d/\lambda 0=0.8}$ is the directivity of a 1*8 subarray along x-direction with spacing d/λ_0 =0.8. It can be seen that when spacing d/λ_0=0.7, the directivity of the array is reduced by 0.5dB compared with the directivity of the array with spacing d/λ_0=0.8; when spacing d/λ_0=0.57, the directivity of the array is reduced by 1.32dB compared with the directivity of the array with spacing d/λ_0=0.8.

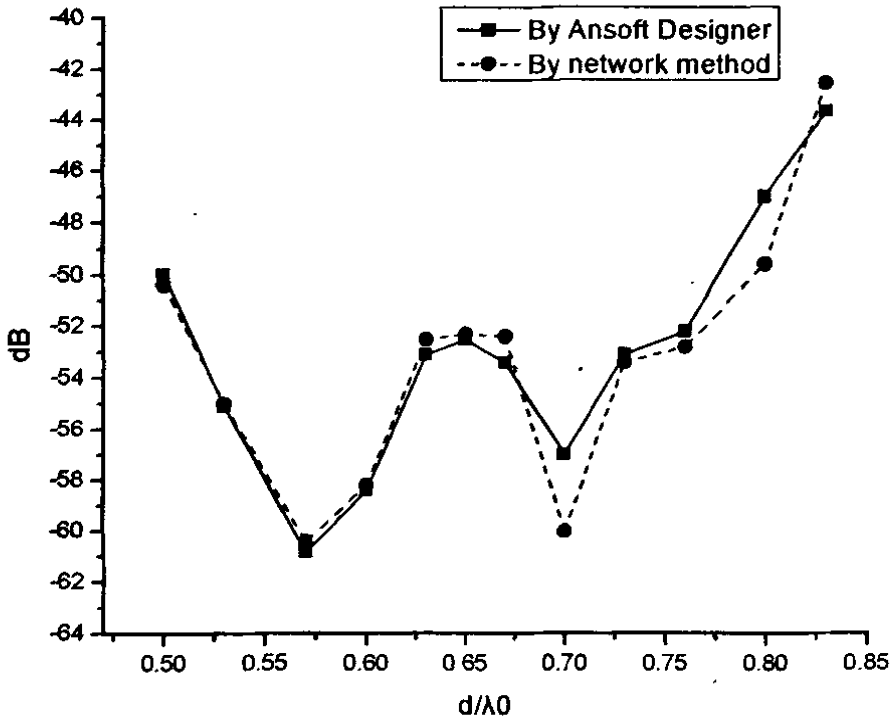

Fig.4.9. The comparison of S_{21} parameters calculated by Ansoft Designer and network method for different spacings.

Table.4.3. The variation of directivity for different spacings.

d/λ_0	ΔD(dB)	d/λ_0	ΔD (dB)
0.83	0.07	0.63	-0.87
0.8	0	0.56	-1.10
0.87	-0.14	0.57	-1.32
0.83	-0.32	0.53	-1.55
0.7	-0.50	0.5	-1.82
0.67	-0.66		

The reduction of directivity for spacing d/λ_0=0.7 and spacing d/λ_0=0.57 can be explained by the H-plane radiation patterns, which are calculated by formula (4.15) and shown in Fig.4.10. It can be seen that the beamwidth of the pattern with d/λ_0=0.7 is broader than d/λ_0=0.8, while the beamwidth of the pattern with d/λ_0=0.57 is broader than d/λ_0=0.7. Broader beamwidth leads to less directivity. The side lobe levels of the three kinds of spacings are all below -12.5dB.

Considering the mutual coupling as well as the directivity and radiation patterns, the element spacing of the adjusted 8*8 array is set to be d/λ_0=0.7.

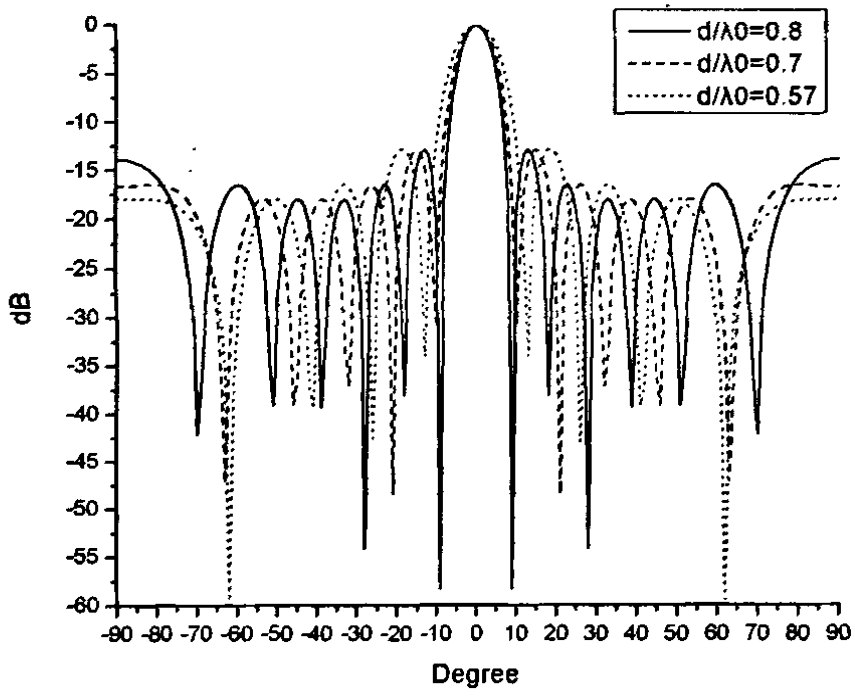

Fig.4.10. The comparison of H-plane radiation patterns for different spacings.

4.4.3 The simulated results of the arrays by Ansoft Designer

The adjusted element spacing is d/λ_0=0.7. In this section, the VSWR, the mutual coupling, the antenna gain and radiation patterns are simulated for the adjusted arrays by Ansoft Designer. And the comparisons are made with the results of the original arrays with spacing d/λ_0=0.8. Fig.4.11 shows the layout of the two adjusted arrays.

Fig.4.12 shows the VSWR of the original design and the adjusted design calculated by Ansoft Designer. The simulated bandwidth is broader than 10% (for VSWR<2). The feeding network of the adjusted design is slightly adjusted to obtain a good VSWR.

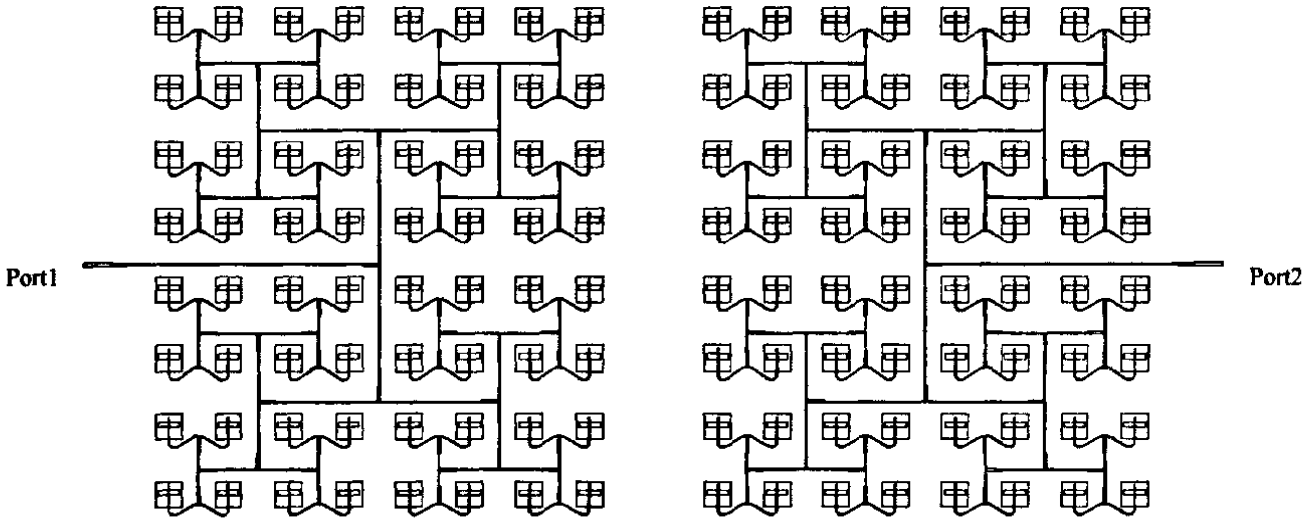

Fig.4.11. The layout of the two adjusted arrays.

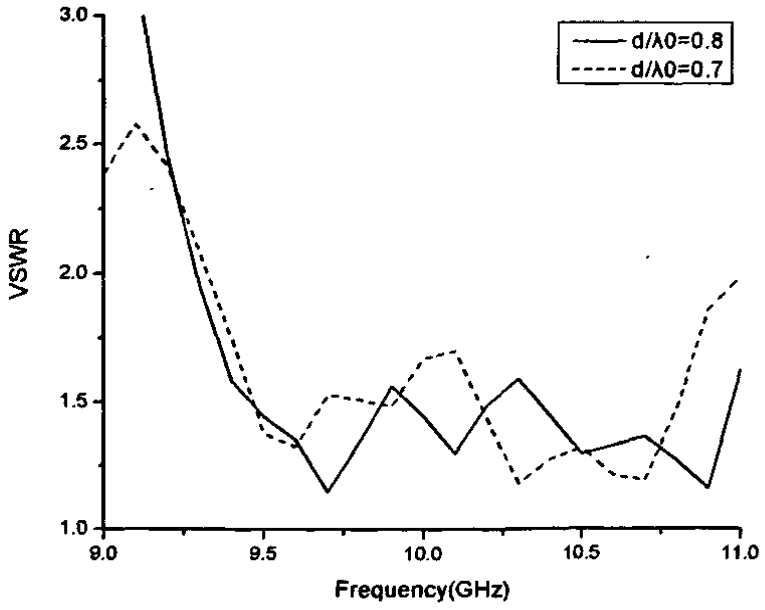

Fig.4.12. The VSWR of the original design and the adjusted design.

Fig.4.13 shows the S_{21} parameter of the original design and the adjusted design calculated by Ansoft Designer. It is seen that the mutual coupling is reduced from -47dB to -57 dB at center frequency 10GHz when the element spacing is changed from d/λ_0=0.8 to d/λ_0=0.7, which agrees well with the network method. The mutual coupling is reduced by 10 dB across a 10% bandwidth.

Fig.4.14 and Fig.4.15 show the calculated H-plane and E-plane radiation patterns of the original design and the adjusted design by Ansoft Designer, respectively. It is seen in Fig.14 that the beamwidth of the H-plane pattern with spacing d/λ_0=0.8 is broader than the beamwidth of the H-plane pattern with spacing d/λ_0=0.7, which will lead to the decrease of gain. The simulated gain of an 8*8 array with spacing d/λ_0=0.8 is 25dB at 10GHz, while that of an 8*8 array with spacing d/λ_0=0.7 is 24.5dB. The gain is decreased by 0.5dB, which agrees well with the results obtained by formula (4.20). The E-plane radiation patterns of both arrays are similar with each other, as is shown in Fig.4.15. This is because the element spacing is not changed during the optimization. The side lobe levels are below -12.5dB for both of the two kinds of element spacings.

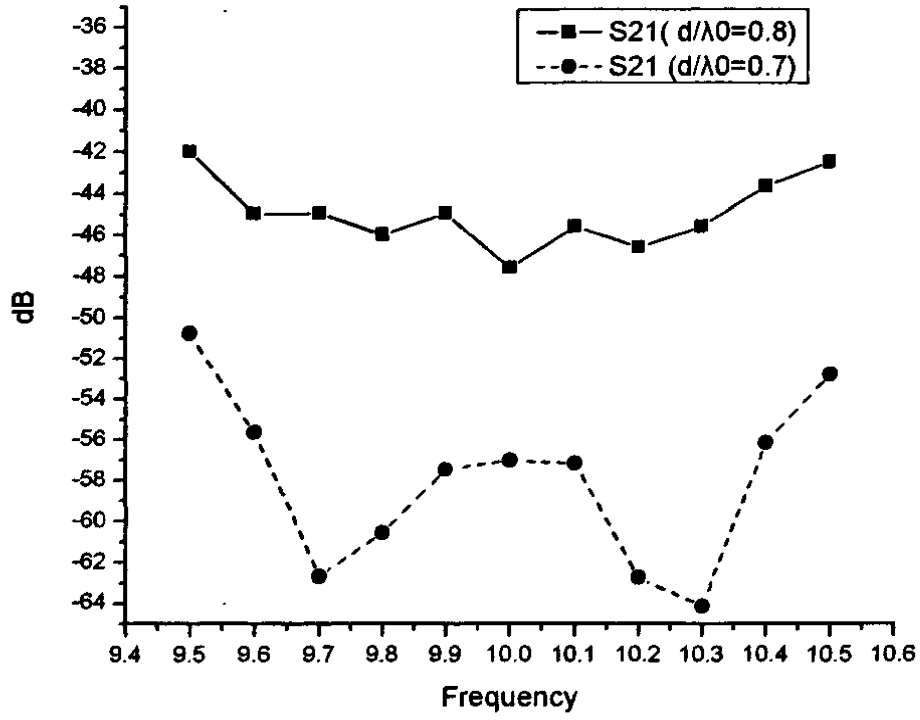

Fig.4.13. The mutual coupling parameters of the original design and the adjusted design by Ansoft Designer.

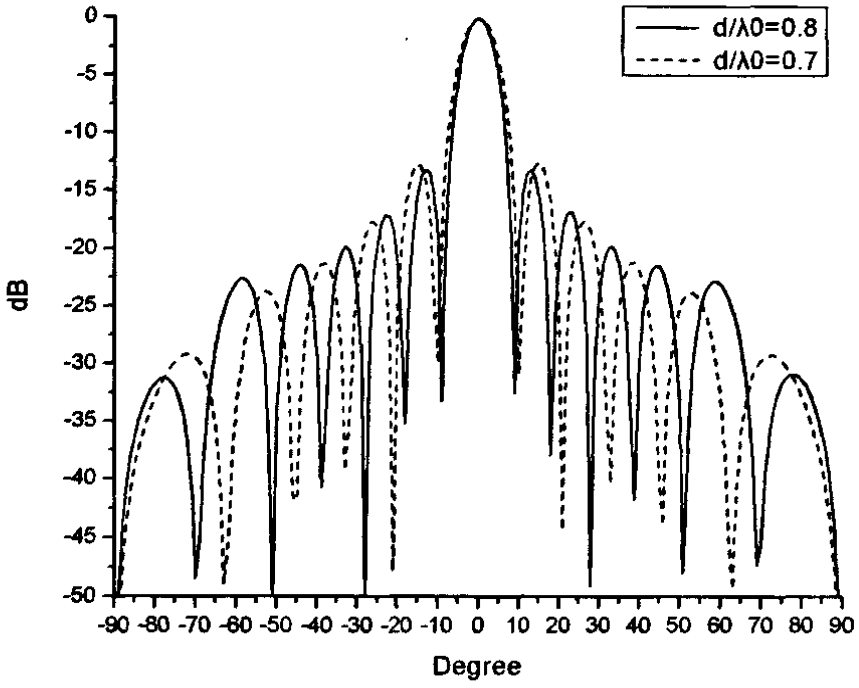

Fig.4.14. The H-plane radiation patterns of the original design and the adjusted design by Ansoft Designer

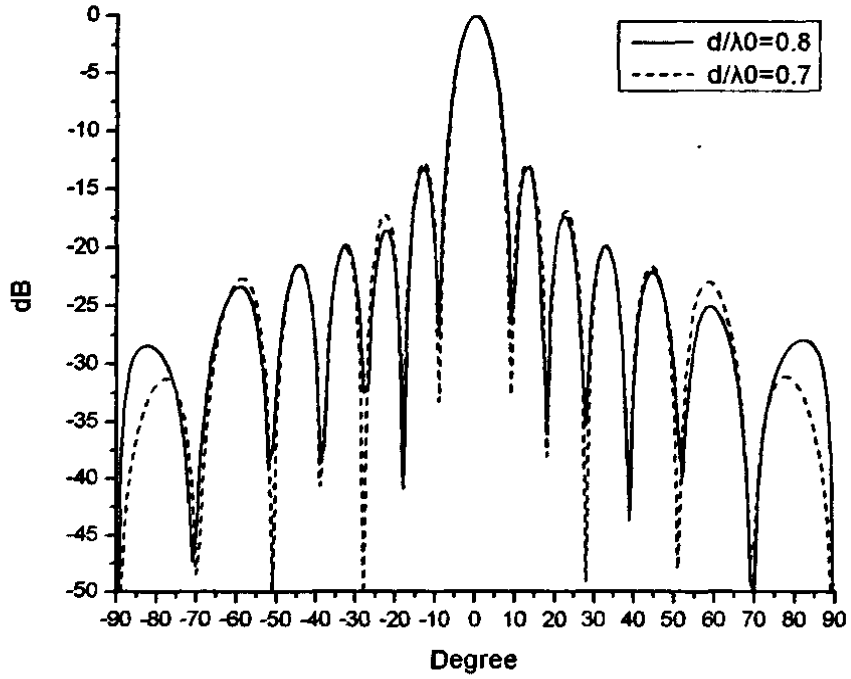

Fig.4.15. The E-plane radiation patterns of the original design and the adjusted design by Ansoft Designer

4.4.4 Measured results

Two 8*8 H-plane coupled microstrip arrays with spacing d/λ_0=0.8 are fabricated and tested. For comparison, two 8*8 arrays with spacing d/λ_0=0.7 are fabricated and tested too. Fig 4.16 shows the measured return loss. The two curves are a little different, because the feeding networks are slightly adjusted to obtain a good return loss for different kinds of element spacing. Neglecting the difference, both of the two kinds of arrays have a bandwidth larger than 10% (for S_{11}<10dB).

Fig 4.17 shows the simulated and measured gain against frequency for element spacing d/λ_0=0.8 and d/λ_0=0.7. The measured gain at 10GHz of an 8*8 array with element spacing d/λ_0=0.8 is 24.5dB, while that of an 8*8 array with element spacing d/λ_0=0.7 is 23.8dB. A 0.7dB gain decrease is measured at 10GHz, while the simulated decrease is 0.5dB. The measured gain of the array with element spacing d/λ_0=0.8 is above 23.8dB across the 10% bandwidth (9.5GHz to 10.5GHz). The measured gain of the array with element spacing d/λ_0=0.7 is above 23.1dB across the 10% bandwidth (9.5GHz to 10.5GHz).

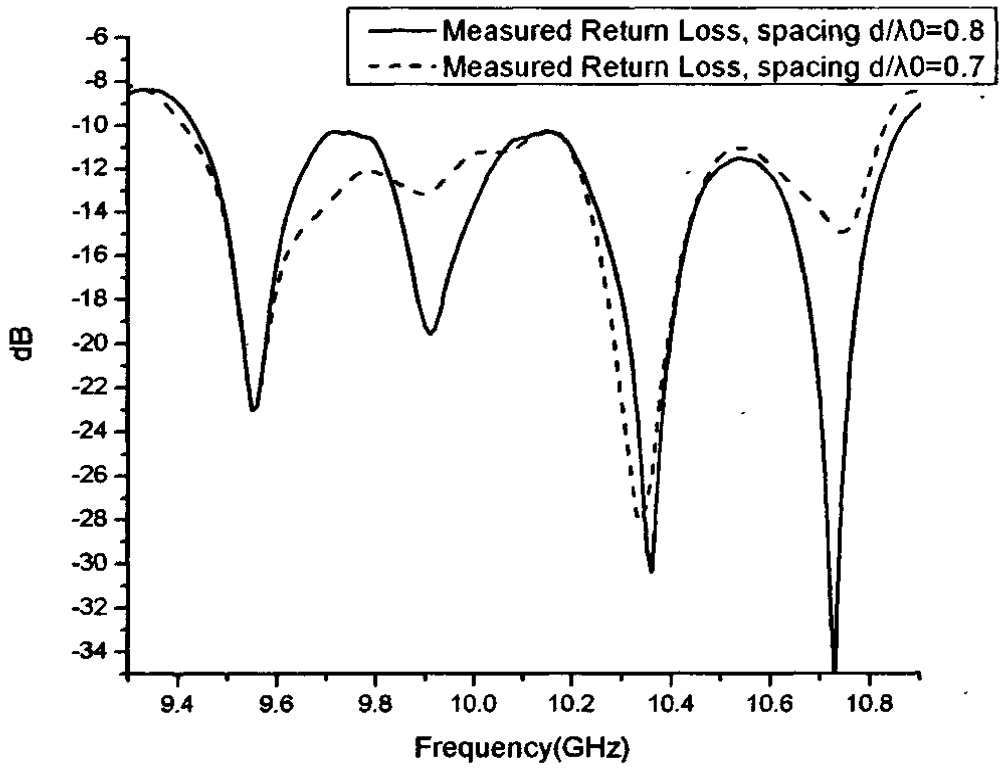

Fig.4.16. measured return loss

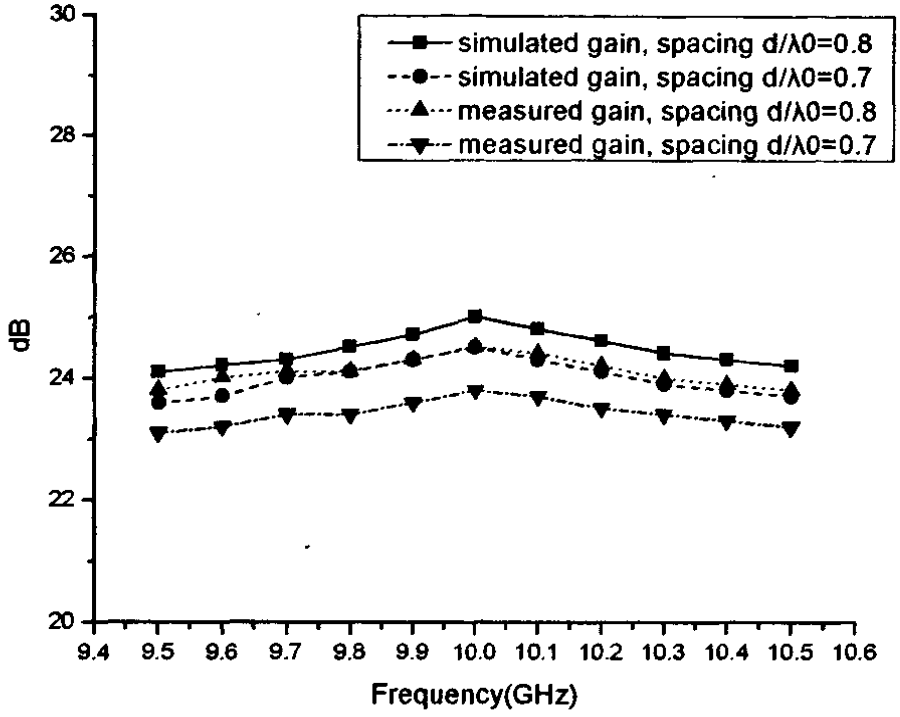

Fig.4.17. simulated and measured gain against frequency

Fig.4.18 shows the simulated and measured S_{21} parameters. The measured mutual coupling level of the arrays with element spacing d/λ_0=0.8 is -43.67dB at 10GHz, while that of the arrays with element spacing d/λ_0=0.7 is –57.67dB. The measured mutual coupling level of the arrays with element spacing d/λ_0=0.7 is below -52.2dB across the 10% bandwidth. The reduction of mutual coupling is at least 10dB at each measured frequency point from 9.5GHz to 10.5 GHz.

Fig 4.19 and 4.20 shows the measured H-plane and E-plane radiation patterns at 10GHz, respectively. It can be seen in Fig.4.19 that the beamwidth of the array with element spacing d/λ_0=0.7 is broader than that of the array with element spacing d/λ_0 =0.8, which leads to the decrease of gain. The measured side lobe levels of the array with element spacing d/λ_0=0.8 are below -12.9dB, while the measured side lobe levels of the array with element spacing d/λ_0=0.7 are below -12.6 dB.

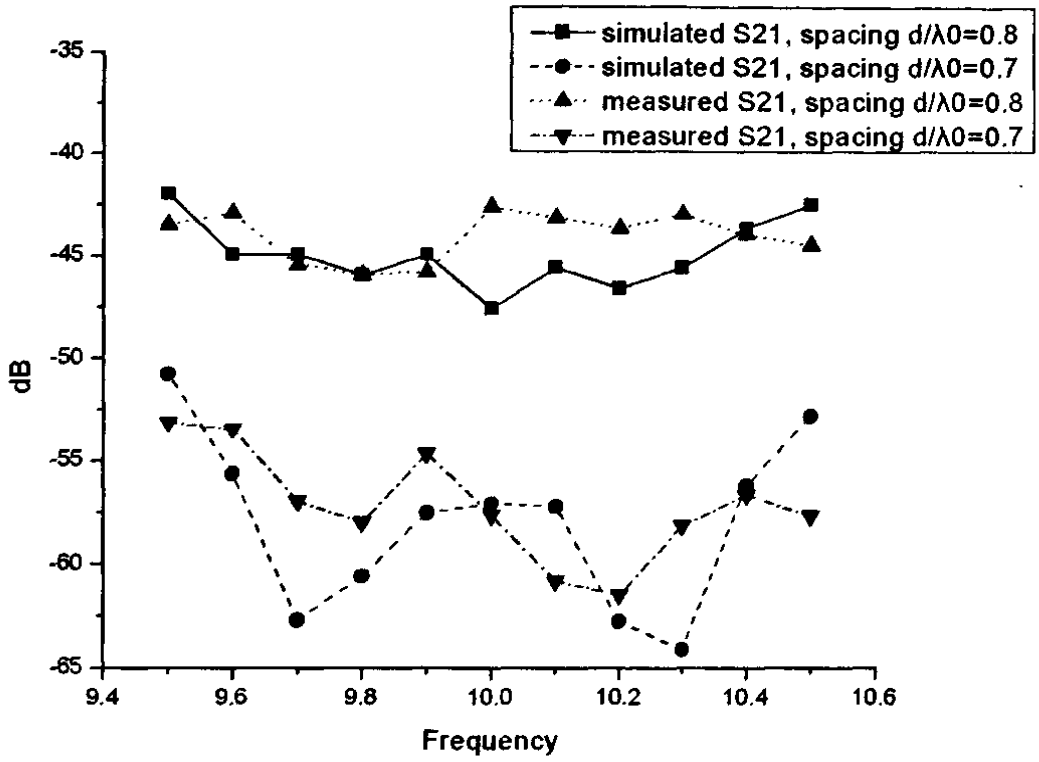

Fig.4.18. simulated and measured S_{21} parameters.

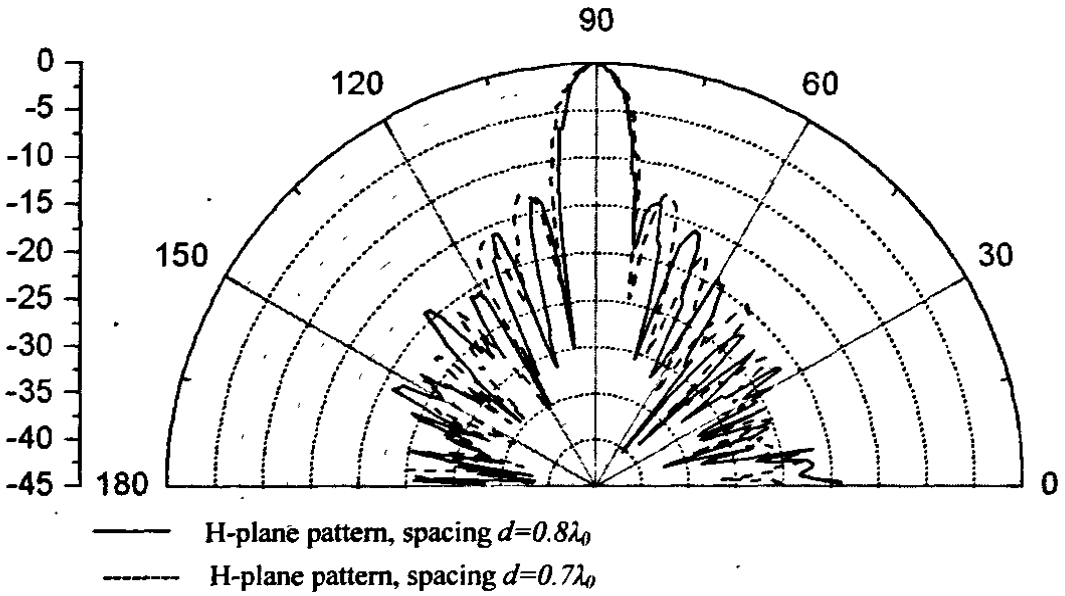

Fig.4.19. measured H-plane radiation pattern

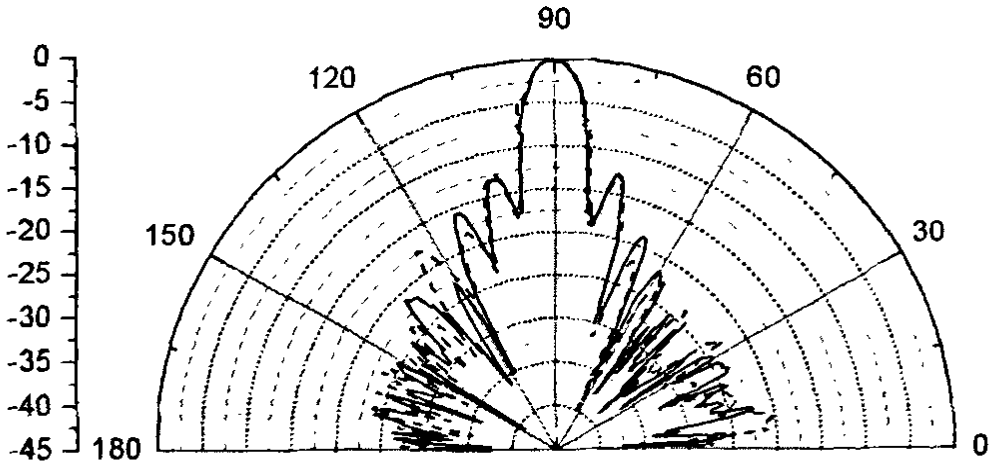

Fig.4.20. measured E-plane radiation pattern

4.5 Conclusion

Reduction of the mutual coupling between the arrays is very important for the continuous wave radar. It was found that the full wave analysis is a must to obtain the correct results. The full wave based network method is introduced to calculate the mutual coupling between two aperture coupled antenna arrays. This method separates the array into two parts: the radiating elements and the feeding networks. The scattering parameters of the radiating elements are obtained by the in-array mutual impedance formula, while the scattering parameters of the feeding network are calculated by the full wave solver Ansoft Designer. This method can reduce the calculating time from 180 minutes to 30 minutes.

The mutual coupling reduction between two arrays through adjusting the element spacing is effective and practical. The mutual coupling levels of different kinds of element spacings are calculated by the network method. The 10dB reduction of mutual coupling is achieved between the original design and the adjusted design in bandwidth of 10% without the significant decrease of the gain, and the degradation of side lobe levels (SLLs), and the VSWR bandwidth. The good agreement is observed between the simulated and the measured results. If the element is chosen carefully and the perfectly conducting fence is placed and adjusted between two arrays, the mutual coupling between two arrays is expected to reduce further.

5 Conclusion

This thesis includes three main parts: the design of a novel broad microstrip antenna, the reduction of mutual coupling between antenna elements using parasitic structure, and the calculation and reduction of mutual coupling between antenna arrays.

A novel fork-like stripline-fed aperture coupled antenna element is designed and tested. The structure is fully planar and includes two layers of ground planes. By using the fork like feeding line, a broad bandwidth is obtained. The nonresonant apertures are used to reduce the backlobe level.

The reduction of mutual coupling between two microstrip antennas is presented. By using a novel parasitic structure, a broadband reduction of mutual coupling is obtained. The parasitic structure has little effect on the antenna radiation patterns.

The network method is used to calculate the mutual coupling between two 8*8 aperture coupled antenna arrays. It is shown that full wave analysis is a must when analyzing the mutual coupling between arrays. The network method uses the full wave based in-array impedance formula to give the scatter parameters of the radiating elements. The scatter parameters of the feeding network are calculated by Ansoft Designer. By using an easy cascade of the two parameter modules, the mutual coupling between two arrays is obtained. The calculation time is reduced from 180 minutes to 30 minutes. The array element spacing is adjusted to reduce the mutual coupling. The mutual coupling between adjusted arrays shows a 10dB reduction compared with that of the origin design across a 10% bandwidth.

Acknowledgements

I would like to express my most sincere appreciation to my dedicated supervisor, Prof. Fang Dagang, for his professional and patient guidance. He has given me a lot of valuable advice, novel ideas and guidance, which have helped me in solving many key problems in my research. From him I not only learned the advanced theory in Electromagnetic area but also the way to be a successful researcher: honest, diligence, team spirit and creativity. Also, I was taught that the value of education lies in its application to daily life.

I would also like to thank Prof. Sheng Weixing and Prof. Dai Yongsheng for their help.

Chapters 2 and 4 are the results of the collaboration with Mr. Wang Hao. The author shares his thanks to him for his guidance and help in my research. Mr. Yu Wenming receives my gratitude for their help in computer programming. Thanks also go to Mr Huang Xiaobo and Ms. Zhang Aijuan for their help in carrying out the measurement. To all other friends and colleagues at Microwave and Millimeter Wave Laboratory who contributed to this thesis in one way or another, I want to express my deepest appreciation and respect.

Last, but never least, I would like to dedicate this work to my family. Their patience, understanding, and sacrifice which they have offered during my course of study are valuable beyond measure, and they are my always inspiration.

References

[1] G. A. Deschamps, "Microstrip microwave antennas," 3rd USAF symposium on Antenna, 1953.

[2] W. J. Lui, C. H. Cheng, Y. Cheng, H. Zhu, "Frequency notched ultra-wideband microstrip slot antenna with fractal tuning stub," *Electronics Letters*, vol.41, no.6, 17 March 2005, pp. 294- 296.

[3] J. –F. Zurcher, and F. E. Gardiol, *Broadband Patch Antennas*, Artech House, Norwood, MA, 1995.

[4] R.Zhang, D.G.Fang, K.L.Wu and W.X.Sheng, "Study on the Elimination of Surface Wave by Metal Fences," Proceedings. Asia-Pacific Conference on Environmental Electromagnetics, CEEM'2000, pp.174-178.

[5] D. M. Pozar, "Microstrip Antenna Aperture-Coupled to a Microstrip Line," *Electronics Letters*, vol. 21, Jan.1985, pp. 49-50.

[6] F. Croq, A. Papiernik, "Stacked slot-coupled printed antenna," *IEEE. Microwave and Guided Wave Letters*, vol.1, no.10, Oct 1991, pp. 288-290.

[7] S. D. Targonski, R. B. Waterhouse, and D. M. Pozar, "Wideband aperture coupled stacked patch antenna using thick substrates," *Electronics Letters*, vol.32, no.21, 10 October 1996, pp. 1941-1942.

[8] Wei Chen, Kai-Fong Lee, R. Q. Lee, "Spectral-domain moment-method analysis of coplanar microstrip parasitic subarrays," *Microwave and Optical Technology Letter*, vol. 6, no. 3, 03/1993, pp. 157-163.

[9] Jiang Xiao, Ge Dong, and MinHui Zhu, "A Novel Aperture Coupled Microstrip Antenna Array with Low Cross-Polarization, Low Sidelobe and Backlobe," Microwave and Millimeter Wave Technology, 2004. ICMMT 4th International Conference on, Proceedings, 18-21 Aug. 2004, pp. 223-226.

[10] Wansuk Yun, Young-Joong Yoon, "A wide-band aperture coupled microstrip array antenna using inverted feeding structures," *IEEE Trans. Antennas Propag.*, vol. 53, no. 2, Feb. 2005, pp. 861- 862.

[11] B. A. Brynjarsson, T. Syversen, "Cavity-backed, aperture coupled microstrip patch antenna," Eighth International Conference on Antennas and Propagation, vol.2, 1993, pp. 715-718

[12] Targonski, D. M. Pozar, R. B. Waterhouse, "Aperture-coupled microstrip antennas using reflector elements forwireless communications," IEEE-APS Conference on Antennas and Propagation for Wireless Communicationss, 1998, pp. 163-166.

[13] A.Bhattacharyya, O. Fortham, and Y. Liu, "Analysis of stripline-fed aperture-coupled patch antennas with vias for parallel-plate mode suppression," *IEEE Trans. Antennas Propag.*, vol.46, no.4, 1998, pp. 538–545.

[14] P. Brachat., and J. M. Baracco., "Dual-polarization aperture-coupled printed antennas fed by stripline," *IEEE Trans. Antennas Propag.*, vol.43, no.7, 1995, pp. 738–742.

[15] C. Chen, W. E. Mckinzie, and N. G. Alexopoulos, "Stripline-fed arbitrarily shaped printed-aperture antennas," *IEEE Trans. Antennas Propag.*, vol. 45, no. 7, 1997, pp. 1186–1198.

[16] J. M. Baracco and P. Brachat, "Shielded microstrip subarray with large bandwidth and low cross polarization," IEEE AP Symp., Chicago, July 1992.

[17] K. Wincza, S. Gruszczynski and K. Sachse, "Aperture coupled to stripline antenna element for integrated antenna arrays," *Electronics Letters*, vol. 42, no. 3, pp.130-131, February 2006.

[18] R.P. Jedlicka, M.T. poe, and K.R. Carver, "Measured mutual coupling between microstrip antennas," *IEEE Trans. Antennas Propag.*, vol. 29, no.1, Jan 1981, pp. 147-149.

[19] E. Penard and J.-P. Daniel, "Mutual coupling between microstrip antennas," *Electronics Letters*, vol.18, no.14, July 1982, pp. 605-607,

[20] D.M. Pozar, "Input Impedance and Mutual Coupling of Rectangular Microstrip Antennas," *IEEE Trans. Antennas Propag.*, AP-30 (6), 1982, pp.1191-1196.

[21] T. Huynh, K. –F. Lee, S. R. Chebolu, R. Q. Lee, "Mutual coupling between rectangular microstrip patch antennas," Antennas and Propagation Society International Symposium, 1992.AP-S.1992, 18-25 Jul 1992, pp.1186-1189 vol.2.

[22] R.Fralich, J.Wang, J.Litva, "Mutual coupling of two microstrip line-fed patch antennas," Antennas and Propagation Society International Symposium, 1989. AP-S. Digest, 26-30 Jun 1989, pp.430-433 vol.1.

[23] J.R.Mosig and F.E.Gardio, "A Dynamical Radiation Model for Microstrip Structures," *Advances in Electronics and Electron Physics*, 1982, vol. 59.

[24] A.F.Muscat, C.G.Parini, "Mutual coupling in aperture fed patch antennas: theory and experiment," Antennas and Propagation, 1999. IEE National Conference on, Aug 1999, pp. 359-362.

[25] A.Taflove, *Computational Eletrodynamics–The Finite-Difference Time-Domain Method*, Artech House Inc., Boston, USA, 1995.

[26] D. M. Sheen, S. M. Ai, M. D. Abouzahra, and J. A. Kong, "Application of the Three Dimensional Finite-Difference Time-Domain Method to the Analysis of Planar Microstrip Circuits," *IEEE Transactions on Microwave Theory and Techniques*, vol. 38, no. 7, 1990, pp. 849-857.

[27] U. K. Revankar, A. Kumar, "Mutual coupling between stacked three-layer circular microstrip antenna elements," *Electronics Letters*, vol.30, no. 24, 24 Nov. 1994, pp.1997-1999.

[28] W. Y. Tam, A. K. Y. Lai, K. M. Luk, "Mutual coupling between cylindrical rectangular microstrip antennas," *IEEE Trans. Antennas Propag.*, vol.43, no.8, Aug 1995, pp.897-899.

[29] D. R. Jackson, J. T. Williams, A. K. Bhattacharyya, R. L. Smith, S. J. Buchheit and S. A. Long, "Microstrip patch designs that do not excite surface waves," *IEEE Trans. Antennas Propag.*, vol.41, no.8, Aug. 1993, pp. 037-1360.

[30] A.Khayat, J. T. Williams, D. R. Jackson, and S. A. Long, "Mutual Coupling Between Reduced Surface Wave Microstrip Antennas," *IEEE Trans. Antennas Propag.*, vol.48,

no.10, Oct. 2000.

[31] J.-G. Yook and L. Katehi, "Micromachined Microstrip Patch Antenna with Controlled Mutual Coupling and Surface Waves," *IEEE Trans. Antennas Propag.*, vol.49, Sep. 2001, pp.1282-1289.

[32] Marija M. Nikolic, Antonije R. Djordjevic, and Arye Nehorai, "Microstrip Antennas With Suppressed Radiation in Horizontal Directions and Reduced Coupling," *IEEE Trans. Antennas Propag.*, vol. 53, Nov. 2005, pp. 3469-3476.

[33] M. A. Khayat, J.T. Williams, D. R. Jackson, and S. A. Long, "Mutual coupling between reduced surface-wave microstrip antennas," *IEEE Trans. Antennas Propag.*, vol. 48, Oct. 2000, pp. 1581-1593.

[34] Jackson, J.T. Williams, A. K. Bhattacharyya, R. L. Smith, S. J. Buchheit, and S. A. Long, "Microstrip patch designs that do not excite surface waves," *IEEE Trans. Antennas Propag.*, vol. 41, Aug. 1993, pp. 1026-1037.

[35] S. D. Cheng, R. Biswas, E. Ozbay, S. McCalmont, G. Tuttle, and K. –M. Ho, "Optimized dipole antennas on photonic bandgap crystals," *Appl. Phys. Lett.*, vol.67, Dec.1995, pp.3399-3401.

[36] R. Coccioli and T. Itoh, "Design of photonic band-gap substrates for surface wave suppression," Proc. IEEE MTT-S Symp., 1998, pp.1259-1262.

[37] Ang Yu, Xuexia Zhang, "A novel 2-D electromagnetic band-gap structure and its application in micro-strip antenna arrays," Microwave and Millimeter Wave Technology, 2002. International Conference on 17-19 Aug. 2002, pp. 580- 583.

[38] Li Yang, Mingyan Fan, Fanglu Chen, Jingzhao She, Zhenghe Feng, "A novel compact electromagnetic-bandgap (EBG) structure and its applications for microwave circuits Microwave Theory and Techniques," *IEEE Trans. Antennas Propag.*, vol. 53, no.1, Jan. 2005, pp. 183- 190.

[39] J. P. Daniel, "Reduction of mutual coupling between active monopoles Application to superdirective receiving arrays," *IEEE Trans. Antennas Propag.*, vol. 25, no. 6, Nov 1977, pp. 737- 741.

[40] Qiulin Huang, Xiaowei Shi, "Depressing mutual coupling between patch antennas using multi-layer dielectric boards," Antennas and Propagation Society International Symposium, 2003. IEEE, vol.1, 22-27 June 2003, pp. 622- 625.

[41] K. Buell, H. Mosallaei, K. Sarabandi, "Electromagnetic metamaterial insulator to eliminate substrate surface waves," Antennas and Propagation Society International Symposium, 2005 IEEE, vol. 2A, 3-8 July 2005, pp. 574- 577.

[42] J.-P. Ho, J. Ji-Yong Park C. Caloz, T. Itoh, "A compact subdivided microstrip square patch array with low mutual coupling," Antennas and Propagation Society International Symposium, 2003. IEEE, vol.1, 22-27 June 2003, pp. 589- 592.

[43] J. P. Gianvittorio, Y. Rahmat-Samii, "Fractal element in array antennas, investigating reduced mutual coupling and tighter packing," Antennas and Propagation Society International Symposium, 2000. IEEE, vol.3, 07/16/2000-07/21/2000, pp.1704-1707.

[44] H. Xin, K. Matsugatani, M. Kim, J. Hacker, J.A. Higgins and M. Rosker and M. Tanaka, "Mutual coupling reduction of low-profile monopole antennas on high-impedance ground plane," *Electronics Letters*, vol. 38, no. 16, Aug. 2002, pp. 849-850.

[45] Kyeong-Sik Min, Dong-Jin Kim and Young-Min Moon, "Improved MIMO antenna by mutual coupling suppression between elements," Wireless Technology 2005.The European conference on 3-4 Oct. 2005, Oct. 2005, pp.125 – 128.

[46] Y. X. Sun, Y. L. Chow, and D. G. Fang, "Mutual Impedance Formula Between Patch Antennas Based on Synthetic Asymptote and Variable Separation," *Microwave Opt. Technol. Lett.*, vol. 35, no. 6, Dec. 2002, pp. 466-470.

[47] M. C. Bailey, *Technique for Extension of Small Antenna Mutual Coupling Data to Larger Antenna Arrays*, NASA Technical Paper 3603, Langley Center, Hampton VA., August 1996.

[48] E.levine, G.Malamud, S Shtrilman, and D.Treves, "A study of microstrip array antennas with the feed network," *IEEE Trans. Antennas Propagat.*, vol.37, no.4, April 1989, pp.426-434.

[49] D. R. Jackson, W. F. Richards and A. Ali-khan, "Series Expansion for the Mutual Coupling in Micriostrip Patch Arrays," *IEEE Trans. Antennas Propagat.*, vol. 37, no. 3, March 1989, pp.269-274.

[50] Y. P. Xi, D. G. Fang, Y. X. Sun and Y. L. Chow, "The Application of Closed-Form Mutual Impedance Formula in the Analysis of the Finite Patch Antenna Array," Proceedings of Asia-Pacific Conference on Environment Electromagnetics, Hangzhou, China, Nov. 2003, pp. 298-301.

[51] D. M. Pozar, "Input Impedance and Mutual Coupling of Rectangular Microstrip Antennas," *IEEE Trans. Antennas Propagat.*, vol. AP-30, no. 6, Nov. 1982, pp. 1191-1196.

[52] Robert J. Mailloux, "Reduction of mutual coupling using perfectly conducting fences," *IEEE Trans. Antennas Propag.*, no. 3, March 1971, pp. 166-173.

[53] D. G. Fang, *Antenna Theory and Microstrip Antennas*, Science Press, Beijing, 2006. .

Papers Completed

1. X. K. Tang, H. Wang, D. G. Fang, "A novel fork-like aperture coupled antenna element," Proceedings of Cross Strait tri-Regional Radiao Science and Wireless Technology Conference, pp.5-6, 2006.
2. .H, Wang, D. G. Fang, X. K. Tang, and Y. L. Chow, "Mutual coupling reduction between two arrays through adjusting the element spacing," Submitted.